UNIVERSITÀ DEGLI STUDI DI GENOVA

DOTTORATO DI RICERCA IN NEUROSCIENZE

Curriculum Neurosciences and Neurotechnologies

Cycle XXXII

Coordinatore Prof. Angelo Schenone

β3 integrin-dependent regulation of SK channel-mediated Ca^{2+}-activated K^{+} currents in intra- and extra-telencephalic cortical pyramidal neurons

Relatore
Lorenzo Cingolani, PhD

Candidato
Carmela Vitale

Anno accademico 2018-2019

Alla mia

“Guerriera della notte”

Table of Contents

1 Abstract

Integrins are cell adhesion heterodimers that mediate cell-cell and cell-extracellular matrix (ECM) interactions. They regulate various cellular functions in the central nervous system such as the localization of ion channels, calcium (Ca^{2+}) homeostasis and synaptic transmission. Impairment of these functions can lead to neurodevelopment disorders such as Autism Spectrum Disorders (ASD). Small-conductance Ca^{2+}-activated K^+ channels (SK channels) are responsible for the medium afterhyperpolarization (mAHP) current (mI_{AHP}) that regulates excitability and firing pattern in many neurons. I investigated firing properties of layer V (LV) pyramidal neurons of the medial prefrontal cortex (mPFC) in WT and *Itgb3*, the murine gene encoding the β3 integrin subunit, KO mice. I could distinguish two populations of pyramidal neurons in LV: extratelencephalic (ET) and intratelencephalic (IT). By using electrophysiological recordings and pharmacology, I identify a mI_{AHP} in both types of neurons and in both genotypes, albeit with different characteristics: mI_{AHP} is larger and faster in ET than in IT neurons; in the *Itgb3* KO, the mI_{AHP} is smaller in ET neurons, as compared to WT. Furthermore, the SK channel-specific blocker apamin affects differently the firing pattern of ET and IT neurons; it increases adaptation in ET neurons, while having no significant effect in IT neurons. To complement the electrophysiological results, I used viral retrograde labelling to investigate expression of β3 integrin and SK channel in both neuronal types. Altogether, my findings indicate that β3 integrin regulates the mI_{AHP} and the firing properties of layer V pyramidal neurons, although to different degrees in ET and IT neurons. These differences might mirror the diverse genetic, anatomy and function of the two neuron subpopulations, allowing them to respond differently to external perturbations that can promote neurodevelopment disorders.

2 Introduction

2.1 Integrins: an overview

Most of the cellular activities of neurons such as the regulation of the action potential firing, synaptic transmission, cell motility and exocytosis are controlled by transmembrane ion fluxes through channels and transporters. These mechanisms depend on the extracellular environment (Morini and Becchetti, 2010), whose variety is communicated to the intracellular signaling pathways by a set of integral membrane proteins that mediate cell-cell and cell-ECM interactions (Hynes, 2002). Among these integral membrane proteins there are integrins, which are cell surface heterodimeric receptors formed by the non-covalent association of α and β subunits (Harburger and Calderwood, 2009). The mammalian genome comprises 18α subunit and 8β subunit genes, which assemble into 24 different functional integrins (Hynes, 2002; Milner and Campbell, 2002). They are expressed in almost every cell of the body, regulating different functions such as cell survival, migration, attachment, focal adhesion assembly and cell differentiation (Campbell and Humphries, 2011) and only a subset of these heterodimers are expressed in the brain, including the hippocampus, cortex, thalamus and cerebellum (Chan et al., 2003; Kerrisk et al., 2014; McGeachie et al., 2011). In particular, several integrin subunits such as α3, α5, α8, αV, β1 and β3 play a variety of roles in the brain regarding neuronal migration, synapse and dendrite development, morphogenesis and stability and synaptic plasticity (Kerrisk et al., 2014; McGeachie et al., 2011). Deficit in integrin function may lead not only to impairments in learning and memory, due to alteration of the neuronal structure, function and synaptic plasticity (Kerrisk et al., 2014), but also to some neurological disorders like ASD (Lilja and Ivaska, 2018) and addiction (Kerrisk et al., 2014). The following first chapters are meant to describe the basic knowledge of integrins, to further process the new information gained from this thesis.

2.2 The integrin family

Integrins are transmembrane proteins characterized by short cytoplasmic tails connected to the actin cytoskeleton and by a large extracellular domain, which forms elongated stalks and globular ligand-binding head regions (Hynes, 2002). The intracellular tails of the β integrin subunits bind to cytoplasmic signaling proteins activating signaling cascades, while the extracellular head domains of the α integrin subunits bind to and provide ligand specificity (Kerrisk et al., 2014). Integrins can be ascribed to different subfamilies, according to their binding to components of the extracellular matrix (Cabodi et al., 2010; Hynes, 2002). Receptors with α5, α8 and αV subunits are considered RGD receptors because they recognize the short motif Arg-Gly-Asp (RGD) in many extracellular ligands, such as fibronectin (FN), vitronectin (VTN), tenascins (TN) and thrombospondins (TSP). Integrins with α1, α2, α10 and α11 are collagen (CN) receptors, while with α3, α6 and α7 integrins subunits bind to the laminin (LM) family proteins (Cabodi et al., 2010; Campbell and Humphries, 2011; Hynes, 2002; Kerrisk et al., 2014; Lilja and Ivaska, 2018) **(Fig. 1)**.

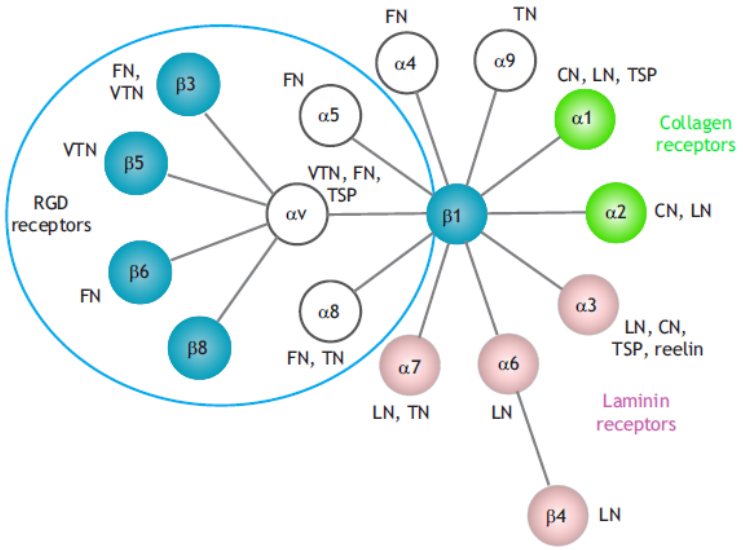

Figure 1. **Integrin family subunits and their receptors.** Integrin heterodimers are classified based on their receptors of the ECM. In the illustration they are represented as an α- and a β-subunit connected by a grey line. Laminin receptors are pink; RGD receptors are shown in the blue circle, and collagen receptors are green. β1 integrin is also a receptor for ICAM-5, CSPG and semaphorin 7A. FN; CN; LN, TN, VTN, TSP (image taken from: (Lilja and Ivaska, 2018).

2.3 Integrin structure, mechanisms of activation and interactions

The three-dimensional structure of the external domain of mammalian integrins was determined on the αVβ3 type (Xiong et al., 2001; Xiong et al., 2002). αV contains four domains: an N-terminal 'β-propeller', a 'Thigh' (Ig-like) domain, Calf-1 and Calf-2 (two β-sandwich domains). The β subunit contains instead eight domains: an N-terminal PSI (Plexin-Semaphorin-Integrin) followed by four EGF-like domains and a tail domain (βTD) close to the plasma membrane; the PSI domain wraps an Ig-like 'Hybrid' domain that contains, between its two β-sheets, the βA domain (Hynes, 2002). The propeller and the βA domains form a 'head', which is thought to account for the formation of the αβ complex **(Fig.2)**.

Before going into the details of integrin activations, it is worth noting that integrin 'inside-out' activation occurs from movement and complete separation of the transmembrane

(TM) segments, whereas ‘outside-in’ activation does not require this separation (Wegener and Campbell, 2008). Thus, TM domains are bonded when inactive and separate when in active state, thus becoming able of binding soluble ligands.

Outside-In activation

During “outside-in signaling”, the binding of ECM to integrins is transduced inside the cells, they undergo a conformational change to properly interact with signaling proteins and to convey information to the nucleus (Hynes, 2002). This allows the polymerization of actin cytoskeleton during cell adhesion and control of cell migration, proliferation, survival and differentiation (Arcangeli and Becchetti, 2010). The known signaling pathways activated during the outside-in signaling include induction of cytosolic kinases, stimulation of the phosphoinositide metabolism, activation of Ras/mitogen-activated protein kinase (MAPK) and Protein kinase C (PKC) pathways and regulation of Rho GTPases (Arnaout et al., 2007; Arnaout et al., 2005). Tyrosine phosphorylation of proteins represents a primary response to integrin stimulation and a preferential way to transduce signals throughout the cell. Among the kinases that are activated and the proteins that are tyrosine phosphorylated upon ECM binding, the Src Family Kinases (SFKs), Focal adhesion kinase (Fak) and the adaptor molecule p130Cas play a prominent role in integrin signaling (Arcangeli and Becchetti, 2010; Harburger and Calderwood, 2009). Upon integrin-mediated adhesion Fak, Src and p130Cas are associated in a multimeric signaling scaffold involved in the organization of Focal Adhesions (FAs), which are sites of close opposition with the ECM. For the regulation of complex processes such as survival, motility, invasion and proliferation, these proteins sustain the organization of FAs, actin cytoskeleton and generation of signaling (Arcangeli and Becchetti, 2010).

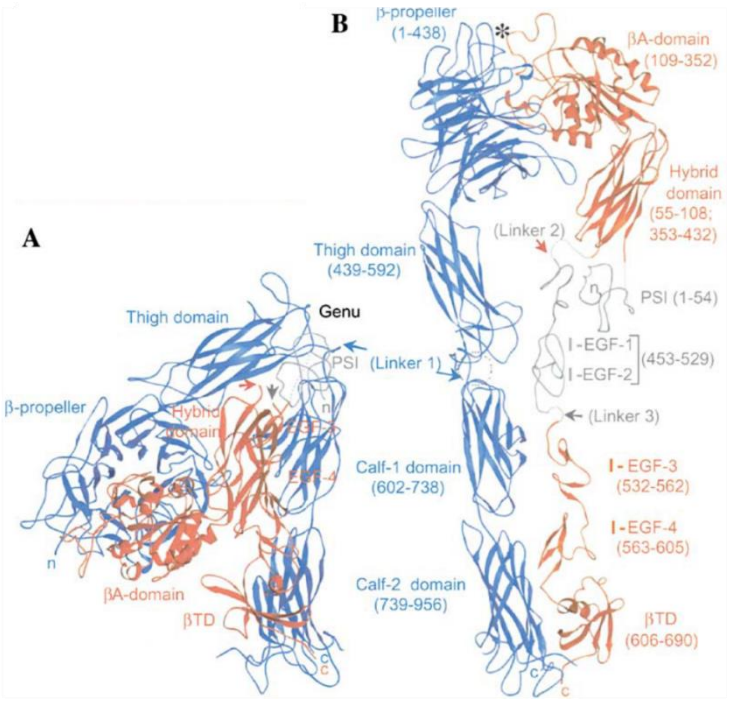

Figure 2.Three-dimensional structure of the αvβ3 integrin (A) The structure of the unliganded αvβ3 is shown as a ribbon diagram with the αv subunit in blue and the β3 subunit in red. In the crystal the integrin is folded over at a bend or "genu," with the head (propeller, β-I/A, and hybrid domains) bent over toward the C termini of the legs which would be inserted into the membrane in an intact integrin. The domains are hard to see in this view and are more readily visualized in (B). **(B)** The structure in (A) has been unfolded by straightening it out at the "genu" of the αv subunit by 135° and rotating the thigh 120° around its axis, with similar adjustments to the β3 structure. The structures of the linker segments (1 in the βv, 2 and 3 in the β3) and of the PSI domain and I-EGF repeats 1 and 2 are not well resolved and are approximate estimates only. The structure reveals two legs extending from the membrane insertion site at the C termini to the head at the top. The head comprises three domains: a β propeller domain at the N terminus of the αv subunit and an I/A domain inserted into a loop on the top of the hybrid domain in the β subunit. The N-terminal PSI domain is curled in below the hybrid domain and is known to be linked by a disulfide bond to the I-EGF-1 repeat, although this connection is not resolved in the crystal structure. The apposition of the propeller and I/A domains is highly similar to that of G proteins. A 310 helix from the I/A domain reaches out to the propeller and inserts an arginine residue into the central channel of the propeller. This arrangement is very similar to the arrangement of a lysine in the α2 helix of the switch II region of Gα inserted into the propeller domain of Gβ. The asterisk marks the loop into which I/A domains are inserted in some integrin α subunits, although not αv. (Image taken from: (Hynes, 2002)

Inside-Out activation

Although the precise structural and topological processes underlying it are still unclear, during the 'inside-out signaling' the activation process is thought to involve the interaction between cytoplasmic ligands and the integrin tails (Harburger and Calderwood, 2009). Hence, a conformational change is triggered and is transmitted to the extracellular ligand-binding domains, through the TM and stalk regions (Arcangeli and Becchetti, 2010). An example of cytoplasmic ligand is the intracellular protein talin (Critchley and Gingras, 2008). Talin can bind to both, the integrin cytoplasmic domains and to vinculin and actin filaments, thus connecting the cytoskeleton and the ECM. In particular, it can bind the cytoplasmic domain of β integrins. The tail head also binds to two signaling molecules that regulate the dynamics of FAs, Fak and the phosphatidylinositol (4)-phosphate-5-kinase type Iγ (PIPKIγ90) (Arcangeli and Becchetti, 2010). Intact talin is relatively inefficient at activating integrins and needs stimulation to trigger significant activation. This implies that their integrin binding sites are masked in the intact molecule. Cleavage of talin by the protease calpain, for example, results in a 16-fold increase in binding to β3 integrin tails (Critchley and Gingras, 2008). A similar effect is also produced by PIP2 binding to talin (Arcangeli and Becchetti, 2010). The talin-mediated integrin activation is stimulated by intracellular messengers such as the small GTPase Rap1A (Bos, 2005). A further mediator of talin activation is the Rap1A-interacting adaptor molecule (RIAM), but other mechanisms for regulating talin and its association with integrins have been suggested (Critchley and Gingras, 2008). As to the 'outside-in' pathways, integrin signaling via Fak and Src promotes binding of PIPK1γ90 to the talin, with ensuing activation of PIPKγ90 and translocation of complex to the plasma membrane. Hence, current evidence suggests that a self-regulating mechanism for activation, depending on integrin-mediated signaling, maintains integrin activation

(Arcangeli and Becchetti, 2010). This mechanism of regulation allows integrins to move from an inactive state, in which they do not bind ligands, to an active state, in which they behave as high affinity receptors. Thus, integrins are capable of bidirectional transmission of mechanical force and biochemical signals across the plasma membrane (Cabodi et al., 2010). Aside from talin, both α and β cytoplasmic tails are known to bind to many other proteins, with consequent mechanical and signaling effects. To date, more than 70 intracellular proteins have been reported to bind integrin tails, with variable specificities (Critchley, 2000; Critchley and Gingras, 2008). Moreover, the β-tail provides multiple protein binding sites containing several ligand-binding sequences. Indeed, the working hypothesis is that the integrin β-tail is the domain involved in the interaction with ion channel proteins (Cherubini et al., 2005). Although the underlying mechanisms of this interaction are still unclear, it has been shown that integrin-mediated cell adhesion in non-neuronal cells stimulates K^+ channel activity (Arcangeli et al., 1993), controls cellular pH and cytosolic free Ca^{2+} (Ingber et al., 1990), thereby affecting cell growth and differentiation (Arcangeli and Becchetti, 2010). This is one of the first proofs showing that integrins can influence the Ca^{2+} influx and K^+ channel activity. Indeed, it would be interesting to investigate the role of integrins in developing neurons. If also in these cells they are able to control the Ca^{2+} influx and the K^+ activity, they would be responsible for important physiological functions.

2.4 Integrins lead to an increase of Ca^{2+} influx

Most of what is known regarding the relations between ligand-gated channels and integrin receptors concerns the mammalian brain. The nervous system develops in progressive stages, all of which depend on ion channel function, often regulated by cell adhesion to the ECM. For example, after each cell division of neural stem cells, neurons migrate

radially or tangentially to reach their final destination (Becchetti et al., 2010a). This process is under complex regulation by ECM proteins, cell–cell adhesion molecules (CAMs), and diffusible factors (Spitzer, 2006; Zheng and Poo, 2007). Once neurons have reached their final location, differentiation occurs, which implies expression of the full complement of voltage-gated channels (VGCs), neurotransmitter synthesis, and expression of neurotransmitter receptors. Moreover, axons must be properly addressed to target tissues for synapse formation; this implies the existence of sensitive mechanisms for regulating growth cone guidance and dendritic outgrowth. Similar Ca^{2+}-dependent signals regulate both dendrite extension during the late stages of neuronal differentiation and the growth cone pathfinding that leads axons to their final postsynaptic targets (Becchetti et al., 2010b). Extracellular cues trigger Ca^{2+} influx through a variety of membrane channels. Ca^{2+} modulates the many well-known calcium-sensitive signalling pathways that converge on cytoskeletal elements and associated regulators such as myosin, Rho, gelsolin and ROCK (Zheng and Poo, 2007). These signals might involve integrins, because of the necessity of coordinating the adhesion site turnover, that is, assembly at the front and disassembly at the rear of moving cells, a particularly delicate mechanism in the long neuronal processes. In the early 1990s, several *in vitro* approaches were applied to the study of the underlying cellular processes and the role of ion fluxes began to emerge. In agreement with the recognition of the importance of Ca^{2+} signals in these processes, neurite growth in response to CAMs was found to depend, at least in part, on activation of voltage-sensitive Ca^{2+} channels (Bixby and Harris, 1991; Doherty et al., 1991). Parallel studies on the integrin-dependent adhesion to the ECM suggested that neurite outgrowth in neuroblastoma cells grown onto FN, VN, or LM depends on activation of K^+ channels, that were subsequently recognized to belong to the K_{v11} subfamily (Becchetti et al., 2010b). In analogy with what has been observed in other cell

types (Arcangeli and Becchetti, 2006), the adhesion machinery could feedback and regulate Ca^{2+}signalling in growth cones as well. Nevertheless, the link between neuronal activity and the expression of membrane receptors that respond to fixed or diffusible guidance cues is still largely unexplored.

Another example, which confirms the increase of intracellular calcium by integrins is due by αv and α6 integrins, which have been found to be necessary for cerebral cortex development, since distinct and severe cortical malformations were observed in murine strains knocked out for these proteins. More recently, the integrin-induced Ca^{2+} fluxes have also been studied in neuron-enriched primary neocortical cultures (Lin et al., 2008a). In these cells, activating α5β1 integrins quickly stimulates a prolonged increase in $[Ca^{2+}]_i$. The response depends on voltage-dependent Ca^{2+} (Cav) channels and N-methyl-D-aspartate receptors (NMDARs), but complete inhibition is only obtained when the voltage-gated Na^+ channels, the α-amino-3-hydroxy-5-methyl-4-isoxazolepropionic acid receptors (AMPARs), and tyrosine kinases are blocked. These and other results suggest that interaction of cultured neocortical neurons with the ECM acts on tyrosine kinase pathways and stimulates Ca^{2+} influx through different pathways both voltage dependent and independent, such as voltage-gated Ca^{2+} channels, NMDARs and Ca^{2+} release from intracellular stores. The mechanistic details of these results are still matter of debate. However, it is evident from the studies above that integrins play an important role in neuronal migration and synapse formation and maturation, by increasing intracellular Ca^{2+}.

2.5 Integrins in synaptic transmission and plasticity

In general, the cerebral expression of integrins is continuously changing during development because it follows the expression of different ECM environments in the

different stages. However, some receptor forms persist in the adult such as β1, β3, β5, and β8 subunits, particularly in the hippocampal and cortical synapses (Becchetti et al., 2010b).

In mature neuronal circuits, the balance between synaptic stability and plasticity depends on membrane interaction with the ECM. Many integrins are localized specifically at synapses (particularly α3, α5, α8, αV and β1, β3, β8) (Kerrisk et al., 2014). In the late 1990 different lines of evidence pointed to a degree of flexibility in the neuronal interactions with the ECM, with implications for synaptic plasticity and neuronal regeneration (Staubli et al., 1998). In fact, integrin ligands containing RGD motifs were soon found to be able to produce changes in neuronal excitability and Ca^{2+} fluxes within minutes (Wildering et al., 2002). Glutamate receptors, in particular, turned out to be a target of integrin dependent regulation (Gall and Lynch, 2004). This has clear implications for synaptic plasticity, as suggested by early work indicating that interfering with the integrin-mediated adhesion to ECM tends to block long-term potentiation (LTP) in adult rat hippocampal slices (Staubli et al., 1998). Subsequently, other studies demonstrated that integrin inhibition caused significant impairment in LTP in hippocampal slices, when integrin-blocking peptides containing the RGD-motif or function-blocking anti-integrin antibodies were used (Staubli et al., 1990; Xiao et al., 1991). An essential study, described the molecular mechanisms by which integrins may influence LTP. The authors first found that a high probability of glutamate release from immature synaptic boutons correlated with high expression of the NMDAR glutamate receptor subunit epsilon-2 (GluN2B) at postsynaptic sites. As synapses matured, glutamate release probability decreased, while NMDAR subunit composition transitioned to those containing predominantly glutamate NMDA receptor subunit epsilon-1 (GluN2A), which have faster kinetics (Cull-Candy et al., 2001). Essentially, chronic

inhibition of the β3 integrin receptor blocked the maturation of hippocampal synapses, preventing both the decrease in release probability and the switch in NMDAR subunit composition, resulting in hypersensitivity to glutamate, a phenotype representative of more immature hippocampal synapses (Chavis and Westbrook, 2001). Several studies have reported principal roles for integrins in both structural synaptic plasticity and functional synaptic plasticity. In hippocampal slices, LTP was quickly suppressed by application of the disintegrins echistatin, which inhibits β1- and β3-containing receptors, and triflavin, which targets preferentially α5β1 integrin receptors (Kerrisk et al., 2014). Moreover, blocking integrin receptors with RGD peptides induces a twofold increase in the amplitude and duration of NMDA synaptic currents (Cingolani et al., 2008; Lin et al., 2003), and genetic disruption of β1 integrin in mature excitatory neurons reduces selectively LTP (Chan et al., 2006; Huang et al., 2006).

The β3 integrin subunit has been revealed to be a key regulator of homeostatic synaptic plasticity (HSP) (Thalhammer and Cingolani, 2014). When the neuronal network activity is blocked to induce HSP, surface levels of β3 integrin subunits are increased, and HSP itself, but not LTP or long term depression (LTD), are blocked in β3 integrin knockout mice (Cingolani and Goda, 2008; Cingolani et al., 2008; McGeachie et al., 2011). At the synapse, β3 integrin subunits interact directly with the Glutamate ionotropic receptor AMPA type subunit 2 (GluA2) of AMPARs to regulate AMPARs trafficking and synaptic strength (Pozo et al., 2012). Moreover, the inhibition of β3 integrin with echistatin leads to AMPARs endocytosis via a pathway demanding the Rap1 small GTPase, which induces general decrease of synaptic transmission (Cingolani et al., 2008). These studies indicate that integrin β1- and β3-containing receptors have both distinct and overlapping roles in regulating spine morphology, synaptic efficacy and multiple forms of synaptic plasticity (Kerrisk et al., 2014). All together, these results highlight the importance of

integrins in modulating the subunits of different receptors with which they interact to regulate either Hebbian or homeostatic plasticity.

In particular, this thesis is focused on the role of β3 integrin, which is associated in the brain only with αV integrin subunit and is important to control HSP, interacting with the GluA2 subunit of AMPARs (Cingolani et al., 2008). Interestingly, recent data from our lab observed that the β3 integrin subunit is intensely expressed at the soma of cortical layer V pyramidal neurons and that it coimmuno-precipitates with Ca^{2+} activated K^+ channels (unpublished data), which are highly expressed in these neurons (for more detail see below).

2.6 Ca^{2+}-activated K^+ channels: an overview

Ca^{2+} is a ubiquitous second messenger and its cytosolic concentration is solidly controlled through a combination of buffer proteins, Ca^{2+} pumps, and transporters (Stocker, 2004). Ca^{2+}-activated K^+ channels have the widest distribution and are the most understood of ion channels that respond to increases in cytosolic Ca^{2+} (Hille, 1986).

There is a variety of Ca^{2+}-activated K^+ channels that can be divided according to their molecular and pharmacological features. Big-conductance K^+ channels (BK channels) are blocked by low concentrations of tetraethyl ammonium and by a number of specific antagonists (Coetzee et al., 1999). The activity of these channels contributes to the repolarization phase of the spike and to the fast part of the afterhyperpolarization (fAHP) (Faber and Sah, 2003). SK channels have lower single-channel conductance (10–20 pS) and are voltage independent, as they are gated by submicromolar concentrations of intracellular Ca^{2+}. SK channels are expressed in many regions of the central nervous system, and their activity has fast effects on intrinsic excitability and synaptic transmission, being responsible for the mI_{AHP}. A third type, the intermediate-conductance

Ca^{2+}-activated K^+channel (IK channel), is structurally and functionally similar to SK channels and part of the same gene family but is broadly absent in central neurons (Adelman et al., 2012). Among this variety of Ca^{2+}-activated K^+ channels, importance here was given to SK channels, since the biochemical interaction with β3 integrin (unpublished data).

2.7 SK channel classification, structure and pharmacology

SK1, SK2, and SK3 are the three clones identified for SK channels (Kohler et al., 1996). Subsequently, also the fourth member of the family was identified: IK1 (Ishii et al., 1997). SK1, SK2, and SK3 mRNAs are expressed throughout the brain in overlapping yet distinct patterns (Stocker and Pedarzani, 2000), whereas IK1 expression in neurons is more limited. The International Union of Pharmacology has now placed all Ca^{2+}-activated K^+ channels into one gene family, in which they are identified as KCa1.1 (BK channels); KCa2.1, KCa2.2, KCa2.3 (SK1,SK2, and SK3 channels); and KCa3.1 (IK1 channels) (Wei et al., 2005). SK channel subunits share the serpentine transmembrane (TM) topology of voltage-activated K^+ channels, with six TM domains and cytosolic N and C termini. The fourth TM domain, which in voltage-activated K^+ channels is the site to positively charged residues on one face of the predicted α helix and composes the voltage sensor (Catterall, 2010), contains three positively charged residues in SK subunits. However, cloned SK channels reflect their native counterparts in lacking any voltage dependency (Blatz and Magleby, 1986), possessing a relatively small unitary conductance (~10 pS in symmetrical K^+), and being gated solely by submicromolar concentrations of intracellular Ca^{2+}ions (apparent *K*D ~ 0.5 μM) (Kohler et al., 1996). The TM core of the SK channel subunits contains the canonical K^+-selective signature sequence in the pore loop between TM domains 5 and 6. The reversal potential (Sah, 1992) and ionic

selectivity of the apamin-sensitive Ca^{2+}-activated K^+ current are consistent with this structure. Functional SK channels assemble as homomeric tetramers (Kohler et al., 1996). However, different subunits can also co-assemble into heteromeric channels both in heterologous expression systems (Monaghan et al., 2004) and in native tissue (Strassmaier et al., 2005).

Regarding their pharmacology, SK2 is the most sensitive to apamin (EC_{50} ~ 40 pM) (Kohler et al., 1996). Apamin sensitivity is mostly conferred to several amino acids in the outer part of the pore (Lamy et al., 2010). Moreover, recent work shows that apamin binding has higher affinity than the effective blocking potency, indicating that apamin may inhibit SK channel activity not by physically blocking the pore, but rather by functioning as an allosteric inhibitor. In addition, several compounds have been described that can enhance SK channel activity, such as the structurally similar compounds 1-ethyl-2-benzimidazolinone (1-EBIO) and 6,7-dichloro-1*H*indole-2,3-dione 3-oxime (NS309) (Cao et al., 2001). These compounds function by increasing the Ca^{2+}sensitivity of SK channels. In this thesis, apamin was used as blocker, while NS309 as enhancer of SK channels activity. The particularity of these channels is their Ca^{2+}-dependent activation that is based on different Ca^{2+} sources. To discover how β3 integrin might influences the activation of SK channels it is fundamental to understand their mechanisms of Ca^{2+} gating and sources.

2.8 Ca^{2+} gating, trafficking and modulation of SK channels

An increase of intracellular Ca^{2+} activates SK channels, although the pore-forming subunits do not contain an intrinsic Ca^{2+}-binding domain. Instead, the Ca^{2+}gating is ensured by a constitutive interaction between the pore-forming subunits and calmodulin (CaM) **Fig. 3a**. CaM binds to the intracellular domain that follows the sixth TM domain,

the CaM-binding domain (CaMBD), which is highly conserved across the SK family. One CaM is thought to bind each subunit of the tetrameric channel and the binding and unbinding of Ca^{2+} ions to the N-lobe E-F hands of CaM are transduced via conformational changes into channel opening and closure, respectively (Xia et al., 1998). The isolated structure of the CaMBD in complex with Ca^{2+}-CaM confirms a dimeric organization of two CaMBDs and two CaMs, with the N-lobe E-F hands occupied by Ca^{2+}ions. The CaMBDs interact with each Ca^{2+}-carrying CaM, but do not make direct contact with each other. The interaction of CaM with the CaMBD modifies the geometry of the C-lobe E-F hands on CaM, making them unable of chelating Ca^{2+}ions (Schumacher et al., 2001). In a Ca^{2+}-free complex the structure is monomeric and extended, while the structure becomes dimeric in the presence of Ca^{2+} (Schumacher et al., 2004). Altogether, the structures indicate that Ca^{2+}-gating of SK channels induces a transition from an extended tetramer of monomers to a folded dimer of dimers that changes a region of the CaMBD, translating Ca^{2+}-binding into a mechanical force to open the channel gate.

SK channels have activation time constants of 5–15 ms and deactivation time constants of ~50 ms as shown by fast application of saturating Ca^{2+} (10 μM) to inside-out patches (Xia et al., 1998). In accordance with the macroscopic currents, single-channel analysis reported that SK channels are voltage-independent and that their gating is adequately defined by a model with four closed states and two open states, with Ca^{2+}-dependent shifts between the closed states (Hirschberg et al., 1998).

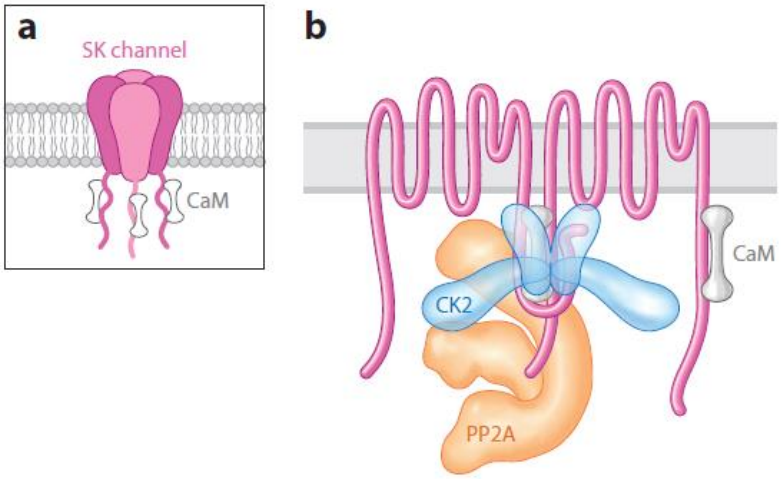

Figure 3. The macromolecular complex of SK channels (a) The structure of SK channels is a tetrameric assembly of the pore-forming subunits, which can be homomeric or heteromeric and have constitutively bound calmodulin (CaM) that mediates Ca^{2+} gating. **(b)** Two of the four subunits of an SK channel are represented. Protein kinase CK2 and protein phosphatase 2A (PP2A) are also constitutive components of the channels. CK2 and PP2A modify the Ca^{2+} sensitivity of the SK channels by phosphorylating or dephosphorylating SK-associated CaM (image taken from: (Adelman et al., 2012). Panel **(b)** is from (Allen et al., 2007).

SK channels present several predicted protein phosphorylation sites (Kohler et al., 1996) and some of these regulate their trafficking. For example, it has been shown in COS cells that protein kinase A (PKA) phosphorylation of serine residues within the C-terminal domain diminishes SK2 plasma membrane expression (Ren et al., 2006). In another study, the PKA phosphorylation of SK channels in amygdala pyramidal neurons reduced the distribution of these channels to the plasma membrane (Faber et al., 2008) and even if the exact sites have not been identified in these cells, such residues are probably the same identified in hippocampal neurons. In CA1 pyramidal neurons, these PKA sites control LTP-dependent trafficking (Lin et al., 2008b). In addition to CaM, SK2 and SK3 channels have constitutively bound protein kinase CK2 and protein phosphatase 2A (PP2A) **Fig. 3b** (Allen et al., 2007). Results from structure-function studies are coherent with a model in which CK2 interacts with multiple domains on the intracellular termini of the pore-

forming subunits, while PP2A is bound by a domain just C-terminal to the CaMBD **Fig. 3b** (Allen et al., 2007). CK2 does not directly phosphorylate the SK2 subunits. Rather, it phosphorylates SK2-bound CaM at threonine 80 [CaM (T80)], but only when the channels are closed, reducing the Ca^{2+}sensitivity of the channels by roughly fivefold. This state dependency of CK2 activity is generated by the relative disposition of a single lysine, K121, in the N-terminal domain of the channels. In the open configuration, PP2A activity dephosphorylates CaM (T80), enhancing the Ca^{2+} sensitivity of the channels (Allen et al., 2007). Therefore, native SK2 and SK3 channels do not have an established Ca^{2+} sensitivity. Rather, the Ca^{2+} sensitivity is Ca^{2+}-dependent, as reflected by the state dependency of modulation. In neurons, this mechanism enhances an activity dependency to SK2 channel activity. CK2/PP2A modulation of native SK channels has been observed in a number of systems. In superior cervical ganglion neurons and dorsal root ganglion neurons, SK channel activity was reduced by noradrenaline and somatostatin, independently of their effects on Cav channels that supply the Ca^{2+} for SK channel gating. The inhibition by these neurotransmitters is CK2-dependent, resulting in phosphorylation of SK-associated CaM and thereby reducing SK channel activity (Maingret et al., 2008). The SK channels have a fascinating way of modulation and trafficking, depending on the mechanisms of phosphorylation/dephosphorilation. Since integrins have been shown to induce the activation of cytosolic kinases and to increase the intracellular Ca^{2+} (trough Cav channels, or NMDARs), it is possible in this way, that the β3 integrins interacting with SK channels could regulate both/or their modulation and the trafficking. To better understand the physiological implications underlying this interaction the activation and the roles of SK channels are described within the following chapters.

2.9 SK channel activation

SK channels are activated by an increase in cytosolic Ca^{2+} coming from several different sources. These are: Ca^{2+} influx via Cav channels; Ca^{2+} influx via Ca^{2+}-permeable agonist-gated ion channels, such as NMDARs and nicotinic acetylcholine receptors (nAChRs); Ca^{2+} released from intracellular Ca^{2+}stores by generation of inositol trisphosphate (IP3) via G protein–coupled receptors, Ca^{2+}- induced Ca^{2+}release (CICR), or a combination of the two. These mechanisms have different cellular distributions and kinetic properties. The activity of SK channel principally follows that of free Ca^{2+} near the channel, indeed the kinetics of the macroscopic current relies on the source and location of Ca^{2+}. Ca^{2+} accessing the cytosol via Cav channels leads to local and large (greater than micromolar) increases in the immediate proximity of the Cav pore, but rapidly equilibrates through a combination of diffusion and buffering (Blaustein, 1988). Cav channels are widely activated during the upstroke of action potentials (APs). Activation of SK channels by inflowing Ca^{2+} is effected by their proximity to Cav channels (Fakler and Adelman, 2008), and their activity follows the time course of changes in free Ca^{2+} in their vicinity. On the other side, Ca^{2+} influx via transmitter-gated channels is slower for their intrinsically slow kinetics. Two Ca^{2+}-permeable ionotropic receptors that are associated with SK channels are NMDARs (Faber et al., 2005) and α9-containing nAChRs (Oliver et al., 2000). In neurons of the hippocampus and amygdala, NMDARs are expressed in dendritic spines, and SK2 channels are found in close apposition. The Ca^{2+} transient activated by synaptic activity is large enough to activate SK2 channels (Sabatini et al., 2002). Notably, in spines, Ca^{2+} influx through NMDARs may not be the main source of Ca^{2+} that activates spine SK channels, whereas, Ca^{2+} influx through α9-containing nAChRs directly and quickly activates nearby SK2 channels (Oliver et al., 2000). Another source of Ca^{2+} is the smooth endoplasmic reticulum; the release of calcium is due to the

activation of IP3 receptors, subsequent to IP3 generation by metabotropic receptor activation. Ca^{2+} ions act cooperatively to activate IP3 receptors, and IP3 generation can interact with AP-induced Ca^{2+} rises to amplify Ca^{2+} release from intracellular stores. This form of Ca^{2+} release activates SK channels (Gulledge and Stuart, 2005). Activation of IP3 receptors and the following release of Ca^{2+} from intracellular stores are intrinsically slow and the Ca^{2+} transients elicited by such release are an order of magnitude slower than those generated by influx from extracellular sources. For example, in midbrain dopamine neurons, both synaptically released glutamate (Fiorillo and Williams, 1998) and ACh (Morikawa et al., 2000) generate a slow inhibitory postsynaptic potential (IPSP) depending on the flow of Ca^{2+} from IP3-sensitive intracellular stores and subsequent activation of SK channels. A similar cholinergic-mediated hyperpolarization is also observed in cortical (Gulledge and Stuart, 2005) and amygdala (Faber et al., 2008) pyramidal neurons. Interestingly, when associated to Ca^{2+} influx via APs, the actions of IP3 on Ca^{2+} release can be enhanced by CICR from IP3 receptors, and store-released Ca^{2+} can elicit an afterhyperpolarization (AHP) that inhibits AP generation (Adelman et al., 2012). Ca^{2+} release from intracellular stores can also arise via ryanodine receptors (RyRs). Hence, in Meynert cells of the nucleus basalis (Arima et al., 2001), ventral midbrain dopamine neurons from young animals and neurons in the medial preoptic hypothalamus, SK channels generate slow spontaneous miniature outward currents that are activated by RyR-mediated Ca^{2+} release from intracellular stores (Adelman et al., 2012). The function of the spontaneous miniature outward currents is still to be understood, but they may affect both spontaneous firing and transitions to burst firing. Furthermore, the spontaneous release of Ca^{2+} from internal stores and the activation of SK channels have been involved in the generation of spontaneous hyperpolarizations in dopamine neurons from neonatal rats (Seutin et al., 2000). In Purkinje neurons, SK2 channel activation is

dependent on P/Q-type Ca^{2+}channel activity, although they may not be directly activated by Ca^{2+} flux through P/Q-type channels. Thus, in Purkinje cells, Ca^{2+}influx through P/Q-type channels is necessary to activate CICR, and in turn, Ca^{2+} ions released from ryanodine-sensitive stores activate SK channels. There are a number of Ca^{2+} sources described, able to increase the intracellular Ca^{2+} activating SK channels. Although it would have been very interesting, the focus of this thesis was not to discover the molecular pathways implicated when β3 integrin was interacting with SK channels, but to analyse how this interaction could interfere with the intrinsic excitability of a neuron.

2.10 The role of SK channels in intrinsic excitability

In many neurons, a single AP or bursts of APs are followed by a prolonged AHP that may depend on Ca^{2+} influx (Stocker, 2004). The AHP controls the intrinsic excitability of neurons and the firing of APs from a given input signal, by two mechanisms. First, the increased K^+ conductance that underlies the AHP following each AP influences the voltage trajectory among APs, thus setting the frequency of cell firing. Second, bursts of APs result in summation of the AHP that ultimately blocks AP firing, a phenomenon known as spike frequency adaptation (Madison and Nicoll, 1982). The AHP may be characterized by different overlapping kinetic components, the fast (f), medium (m) and slow (s) AHPs (Sah, 1996). The fAHP, which overlaps the falling phase of the AP and contributes to spike repolarization and the initial component of the AHP, usually lasts for 10–20 ms (Storm, 1987). The fAHP is frequently due to the activity of BK channels (Storm, 1987). The mAHP activates rapidly and decays over several hundred milliseconds (Stocker, 2004). In many, but not all, cases the mAHP is blocked by apamin, which increases excitability and classifies this AHP component as being due to SK channel activity. A wide variety of neurons have been demonstrated to have an apamin-sensitive

component, including spinal motoneurons, neurosecretory neurons in the supraoptic area of the hypothalamus, vagal motoneurons, pyramidal neurons in the sensory cortex and the lateral and basolateral amygdala, interneurons in the nucleus reticularis of the thalamus (nRt), striatal cholinergic interneurons, hippocampal interneurons in the stratum oriens-alveus and the stratum radiatum, cholinergic nucleus basalis neurons, paraventricular neurons, rat subthalamic neurons, cerebellar Purkinje neurons, noradrenergic neurons of the locus coeruleus, serotonergic neurons of the dorsal raphe, midbrain dopamine neurons, circadian clock neurons in the suprachiasmatic nucleus of the hypothalamus, and mitral cells of the olfactory bulb (Adelman et al., 2012).

The contribution of SK channels to the AHP is mostly due to their activation by Ca^{2+} influx via Cav channels. Nevertheless, in most cases the identity of the Cav channels that increase the intracellular Ca^{2+} and the subtype of the SK channel that contributes to the AHP are not known. Moreover, in those cases in which calcium sources are known, the specific linkage between Cav channels subtypes of SK channels does not seem to be absolutely specific. For example, in cerebellar Purkinje neurons, P/Q-type Ca^{2+} channels are selectively coupled to SK2 channels (Adelman et al., 2012), whereas in their downstream target neurons of the deep cerebellar nucleus, N-type Ca^{2+}channels provide the Ca^{2+} source for SK channel activity (Alvina et al., 2009). Indeed, in some neurons there is more than one functional population of SK channels, which can be coupled to different Ca^{2+} sources. For example, in midbrain dopamine neurons, a slow oscillation of the membrane potential stimulates intrinsic pacemaker activity. The depolarizing phase has been linked to L-type Ca^{2+}channels, while the repolarization phase derives from the activation of SK channels. Instead, the AHP in these neurons is due to Ca^{2+}influx via T-type Ca^{2+}channels, also mediated by SK activity. Similarly, in spinal motoneurons there are two functionally different SK channel populations: one mediates the mAHP and is

activated by Ca^{2+}influx through N- and P/Q-type Ca2+ channels, the other one forms a feedback loop with persistent L-type Ca^{2+}channel currents (Adelman et al., 2012).

Despite the variability in the coupling of Cav channels and SK channels, there is distinct and specific coupling of Ca^{2+} channels to different Ca^{2+}-activated K^+ channels within the same neuron. This is supported by the striking selectivity shown for BK and SK channel activation in acutely dissociated hippocampal neurons. In somatic cell–attached patch recordings, Ca^{2+} influx through L-type channels activates SK channels without activating BK channels that are present in the same patch. The latency between L-type channel and SK channel openings suggests that these channels are 50–150 nm apart. In contrast, Ca^{2+} influx through N-type channels activates only BK channels; opening of the two channel types is almost coincident (Marrion and Tavalin, 1998). The situation is reversed in superior cervical neurons and in vagal motoneurons, in which N-type Ca^{2+} channels provide the Ca^{2+} for SK channels that are responsible for the mAHP while different Cav channels mediate the BK channel activation that underlies the fAHP. This absolute segregation of coupling between channels reflects the strict delineation of submembrane Ca^{2+} microdomains (Adelman et al., 2012). The Ca^{2+} sources that leads to the activation of SK channels are not always known. In this thesis, the SK-mediated current is recorded from the soma of layer V pyramidal neurons of the mPFC, where it has been found that the Ca^{2+} influx through NMDARs, R-type and L-type Ca^{2+} channels as well as Ca^{2+} ions released from IP3-sensitive stores activate spine SK channels. These results indicate that distinct transduction mechanisms might couple with the presence of very restricted Ca^{2+} domains within the spine head (Adelman et al., 2012). Since most of what is known about the function and activation of SK channels is related to their implications in synaptic plasticity and transmission, the following chapter is describing the role of SK channels at synaptic level.

2.11 SK channels: synaptic transmission and plasticity

One of the first proofs showing a direct correlation between SK channels and synaptic plasticity is given by the following paper, reporting that blocking SK channels with apamin during a 5-Hz tetanus enhanced the induction of LTP in area CA1 of the hippocampus (Norris et al., 1998). Later studies demonstrated that apamin influences the induction of synaptic plasticity by reducing the AHP and increasing somatic excitability, either directly in CA1 pyramidal neurons (Kramar et al., 2004; Norris et al., 1998) or indirectly through CA1 interneurons. In spines of pyramidal neurons of the hippocampus and amygdala, SK channels are activated by Ca^{2+} influx coming from synapses and their activity regulates synaptic responses. The activation of synaptic SK channels provides a repolarizing conductance that opposes AMPAR-mediated depolarization, reducing excitatory postsynaptic potentials (EPSPs). Hence, blocking synaptic SK channels with apamin increases EPSPs, this effect can be occluded or reversed by blocking NMDARs before or after apamin application, respectively (Adelman et al., 2012). In particular, most of the Ca^{2+} transient generated in the spine is due to Ca^{2+} influx through NMDARs and in the synaptic membrane of CA1 pyramidal neurons, SK2 and NMDARs are closely colocalized. Nevertheless, the Ca^{2+} source that activates the spine SK channels may not be NMDARs. For example, in one study it has been shown that blocking R-type Cav channels with the peptide toxin SNX-482 is sufficient to block spine SK channel while NMDARs are active. This might suggest that NMDAR activity enhances the depolarization of the spine membrane potential, such a depolarization adds to the AMPAR-mediated depolarization and activates R-type Ca^{2+} channels that sustain SK channel activation (Bloodgood and Sabatini, 2007).

The trafficking of spine SK channels also influences LTP stimulation. At Schaffer collateral to CA1 synapses, LTP induction mobilizes additional glutamate receptor 1

(GluA1)-containing AMPARs to the synaptic membrane, efficiently increasing the depolarizing effect upon excitatory synaptic transmission. On the other side, endocytosis dismisses SK2-containing channels from the synaptic membrane, reducing the normal shunting of the EPSP by these channels. This process implies PKA phosphorylation of serine residues in the C-terminal domain of SK2. Thus, LTP at these synapses depends on the sum of increased AMPARs and decreased SK2-containing channels.

In amygdala pyramidal neurons, β-adrenoreceptor stimulation modulates synaptic SK2 expression by PKA activation. Differently from CA1 pyramidal neurons, SK2 channels are constitutively recycled into and out of the synaptic membrane. In this scenario, PKA selectively interrupts exocytotic delivery of SK channels, enhancing synaptic transmission and plasticity. These studies highlight the importance of synaptic SK2-containing channel localization.

To notice, the modification of neuronal response to synaptic activity may be influenced not only by alteration in synaptic transmission (LTP or LTD), but also by modulation of intrinsic excitability. In this context, the SK channel activity that contributes to the AHP by shaping intrinsic excitability is also subject to activity-dependent plasticity. An example is layer V pyramidal neurons from the rat sensorimotor cortex. Afferent stimulations in the presence of AMPARs and NMDARs blockers lead to an activity-dependent increase of intrinsic excitability (LTP-IE); after stimulation more APs are triggered for a given current injection. The LTP-IE requires metabotropic glutamate receptor 5 (mGluR5) receptor activation and is largely blocked by apamin. Consistently, the mAHP is reduced. In addition, after LTP-IE, spike trains showed fewer failures and greater temporal fidelity, similar to the effects of apamin in the absence of stimulation. On the other hand, enhancing SK channel activity with 1-EBIO had largely opposite effects than apamin (Sourdet et al., 2003).

The functional output of a neuron mirrors the integration of synaptic responses and intrinsic membrane excitability and SK channel activity is involved in both processes. (Adelman et al., 2012). In this regard, our recent review (Cingolani et al., 2019) is suggesting that SK channels might be implicated in the regulation of homeostatic intrinsic plasticity (HIP), which in combination with HSP can contribute to the network stability, when it is perturbed, of different brain regions. β3 integrins are implicated in HSP, it is tempting to hypothesize that, at the level of synapses, the interaction between SK channels and β3 integrin might regulate the homeostasis of the brain networks, controlling the HIP and HSP, respectively. This could be a possible explanation, to confirm it investigation on the homeostasis plasticity need still to be done, since were outside the focus of this thesis. Here instead the interaction between SK channels and β3 integrin has been described analysing the somatic intrinsic excitability of layer V intratelencephalic and extratelencephalic pyramidal neurons of the mPFC in WT and *Itgb3* KO mice.

2.12 Intratelencephalic and extratelencephalic neurons

Deep-layer, pyramidal neurons (DLPNs), are found in layer V and layer VI (LVI) of the neocortex and are a major source of output from the neocortex. Generally, DLPNs can be divided into two classes based on their axonal projections: those with long-range projections confined to the telencephalon: IT and those that also project to other brain regions: ET (Shepherd, 2013) (Baker et al., 2018). Importantly, IT neurons are located to the telencephalon, while ET neurons project both within the telencephalon and beyond. Their specific projection targets can additionally subdivide ET and IT populations. For example, some ET neurons are termed pyramidal tract neurons based on their projection along the white matter tracts in the brainstem. They innervate a variety of brain areas both within and outside of the telencephalon, including the spinal cord, pons, striatum,

brainstem, and/or thalamus (Hirai et al., 2012; Rojas-Piloni et al., 2017). The same diversity stands within IT neuron subpopulations. The projections of some IT neuron populations are confined to the cortical region that they occupy; some project to the claustrum and ipsilateral striatum, while others project across the corpus callosum to contralateral cortex (termed commissural or corticocortical, respectively) and/or to the contralateral striatum (Otsuka and Kawaguchi, 2011; Shepherd, 2013; Wilson, 1987). In the following sections, ET and IT neuron types are described considering the main differentiated characteristics such as molecular and genetic signature, laminar segregation and dendritic arborization, intrinsic excitability and implications in nervous system disorders.

2.13 Molecular signature, laminar segregation and dendritic arborization of deep-layer pyramidal neurons

DLPNs show noteworthy diversity in molecular and gene expression, which may be indicative regarding the mechanisms that govern their development. Differences in gene expression between DLPNs emerge in embryonic development and mediate the specification of projection targets (Lodato et al., 2015; Molyneaux et al., 2007). Several transcription factors determine projection type, Fezf2 (also known as Fezl) and CTIP2 (also known as Bcl11b) are required for the generation of LV corticospinal neurons (Arlotta et al., 2005; Molyneaux et al., 2007). Specification of different DLPN types is driven by several reciprocally repressive transcription factors. Fezf2 and CTIP2 promote LV ET fate by suppressing transcription factors associated with LV IT. Conversely, transcription factors that encourage the specification of LV IT neurons do so through the inhibition of ET-related transcription factors (Alcamo et al., 2008; Muralidharan et al., 2017). Thus, there appears to be correspondence between transcriptomically defined cell

types and the diversity of axonal projections reported in classes of DLPN (Baker et al., 2018). The laminar segregation of projection neurons depends upon cortical region and neuron subtype. Within LV, the somata of ET and most IT neuron populations are distributed through both LVA and LVB (Anderson et al., 2010; Rojas-Piloni et al., 2017). However, one exceptional subtype of ET neuron is restricted to LVB: the corticospinal neuron (Anderson et al., 2010; Baker et al., 2018; Suter and Shepherd, 2015). ET and IT neurons exhibit distinct dendritic morphology, in particular great variability in the apical dendritic arbor is observed. This diversity is at the base of the classification of "thick"- versus "thin"-tufted recognized as useful segregator for ET and IT populations (Ramaswamy and Markram, 2015). On average, the width and/or total dendritic length of the apical tuft distinguishes LV projection neuron types in all cortical regions studied (Dembrow et al., 2010; Joshi et al., 2015; Morishima and Kawaguchi, 2006). The enriched apical arbors of ET neurons relative to IT neurons suggest that ET neurons may integrate many more synaptic inputs arriving at the upper layers and thus may be integrating more inputs from "higher" cortical regions (Baker et al., 2018).

2.14 Intrinsic electrophysiological properties of deep-layer pyramidal neurons

Crucial differences among DLPN populations have been observed for both their subthreshold and suprathreshold properties. Consequently, these neuron populations have the ability to differently integrate information across time. Across cortical areas, LV ET neurons typically display electrophysiological signatures strongly influenced by hyperpolarization-activated nonselective cation (h)-currents (Baker et al., 2018; Dembrow et al., 2010).

Usually, LV ET neurons have a more depolarized resting membrane potential, a faster effective membrane time constant, a lower input resistance, and often display a slow depolarization or "sag" potential in response to hyperpolarization relative to LV IT neurons (Dembrow et al., 2010; Dembrow et al., 2015; Rock and Apicella, 2015; Sheets et al., 2011), even though some exceptions to this properties have been described (Guan et al., 2015; Otsuka and Kawaguchi, 2008). The time-dependent characteristics of h-channels provide distinct filtering properties in LV ET neurons (Anastasiades et al., 2018; Dembrow et al., 2010; Ferreira et al., 2015). ET neurons are most sensitive to sinusoidal current injections at the soma of 3–6 Hz, while IT neurons usually respond to slower (2 Hz) current oscillations (Dembrow et al., 2010).

The filtering properties due to h-channels strongly determine how LV ET neurons integrate incoming synaptic inputs (Anastasiades et al., 2018; Dembrow et al., 2015). Since the different molecular signature of these DLPN populations, it is possible these channels are one main property of this neuronal type. However, the existence of h-channels is not exclusive to LV ET neurons, indeed pharmacological blockade of h-current alters membrane properties of both ET and IT neurons (Dembrow and Johnston, 2014; Kinnischtzke et al., 2016). In general, LV ET neurons have a lower AP voltage threshold than IT neurons, when an AP is triggered, across different cortices (Dembrow et al., 2010; Kalmbach et al., 2015). The rheobase current, or minimal amount of current required to trigger an AP, is depending on a combination of the resting membrane potential, input resistance, and the AP threshold (Baker et al., 2018). Indeed, the amount of steady-state current required to drive APs in LV ET neurons is variable and higher than IT neurons (Baker et al., 2018; Dembrow et al., 2010; Sheets et al., 2011). When active, the firing profile of LV IT neurons shows spike frequency adaptation, with constant current injection the frequency of firing decreases with time, while several ET neurons

display far less adaptation (Crandall et al., 2017; Hattox and Nelson, 2007; Morishima and Kawaguchi, 2006). In some cases, LV ET neurons even exhibit spike frequency acceleration (Dembrow et al., 2010; Oswald et al., 2013). Most likely, these differences are due to singular expressions of voltage-gated potassium channels (Guan et al., 2015; Hattox and Nelson, 2007). Notably, the intrinsic electrophysiological properties of ET and IT neurons are not settled; they can be changed by neuromodulation and plasticity (Baker et al., 2018). Neuromodulators can modify the features of single or sets of ion channels and therefore reshape the dynamic properties of a neuron, generally operating via G-protein-coupled receptors and second messenger cascades. Therefore, understanding how these diverse DLPN subpopulations respond to many neuromodulatory substances remains to be examined.

2.15 Role of deep-layer pyramidal neurons in pathophysiological states

The remarkable variety in genetic, cellular, and functional features of DLPNs places an organized structure for subtype-specific contributions to nervous system disorder. Several subtypes of DLPNs have been implicated in disorders, such as schizophrenia, epilepsy, amyotrophic lateral sclerosis (ALS), and autism spectrum disorders. For example, in a study conducted in mouse models of Fragile X syndrome, the leading recognized genetic cause of autism, the functional expression of several ion channels is altered in LV ET, but not in IT, neurons (Kalmbach et al., 2015; Zhang et al., 2014). As consequence, LV ET neurons in Fragile X syndrome mice are more excitable than in their wild-type counterparts. More interestingly, there is also evidence in non-rodent species for cell type-specific contributions to nervous system disorders. In a monkey model of Parkinson's disease, the in vivo activity of ET neurons is altered, while IT neural activity is almost unchanged (Pasquereau et al., 2016; Pasquereau and Turner, 2011). These are several

examples of many studies that found cell type-specific alterations of neuron function associated with nervous system disorders and indicate the imperative need to develop therapies targeting specific populations of cells for the treatment of nervous system disorders. This would be the ideal long-term goal of the study started in this thesis. Here, the interaction between β3 integrin and SK channels is described exactly in these two neuron types. Interestingly, the literature states that ET are most likely the neurons involved in ASD (see above), on the other hand integrins are also described to play an important role in the development of ASD (see below). Indeed, in the next chapter, more is described about the role of β3 integrin that interact with SK channels in the neurodevelopment, which is the critical step for the onset of ASD.

2.16 β3 integrin and SK channels interplay from the pathophysiological point of view

Important steps of neural development are regulated by early electrical activity and calcium influx (Cingolani et al., 2002). In mature neurons, SK channels regulate action potential firing and shape calcium influx with a feedback regulation (Cingolani et al., 2002; Gymnopoulos et al., 2014). These functions are described in the adult nervous system, but suggest them to be optimal candidates to control activity and calcium dependent processes in neurodevelopment. The possible engagement of SK channels in the regulation of developmental processes is promising due to their early expression in embryonic development. In particular, during the development neurons and neural networks need the combination of gene expression controlled by transcription factors and patterned activity regulated by receptors and ion channels (Gymnopoulos et al., 2014). In this context, the increase of transient calcium, directed by different Ca^{2+}-permeable ligand- and voltage-gated channels, plays an important role. Here integrins come too,

indeed they have been described to control the Ca^{2+} influx and channels activity during the development of neurons. Various aspects of the neuronal development are regulated through Ca^{2+} influx, defined by different spatio-temporal patterns depending on the developmental stage, such as the proliferation of neural progenitors, neuronal migration, axon guidance, neurotransmitter and receptor specification, and synapse formation (Gymnopoulos et al., 2014).

Dysregulation of these processes can lead to impaired neuronal connectivity and increased risk for several neurodevelopmental pathologies, including ASD (Geschwind and Levitt, 2007; McGlashan and Hoffman, 2000). Interestingly, post-mortem studies have shown that synaptic density is decreased in schizophrenia brains, while in autistic brains there is an increase in glutamatergic synaptic spine density (Hutsler and Zhang, 2010; Moyer et al., 2015). Especially, alterations in the molecular components of the postsynaptic density (PSD) of dendritic spines are considered as one of the major etiologies of these disorders (Lilja and Ivaska, 2018). ASD is a disorder that involves deficits in glutamatergic synaptic development and maturation. Interestingly, a study showed that many of the genes discovered to be implicated in ASD, are involved in multiple biological processes at multiple points during development. In this study, the authors determined that a spatio-temporal convergence among groups of disease-related mutations, all known to lead to ASD, has been helpful as a first step toward identifying the functional perturbations relevant for this phenotype. Bearing this in mind, they addressed the key question of if and when, in what brain regions, and in which cell types specific groups of ASD-related mutations converge during human brain development. Their analysis identified robust, statistically significant evidence for convergence of the risk genes in glutamatergic projection neurons in layers V and VI of human midfetal

prefrontal and primary motor-somatosensory cortex (PFC-MSC) around 3-5 postconceptional week (Willsey et al., 2013).

Understanding how ASD-associated genes regulate key cellular pathways in neuronal connectivity could provide important insights and result in more targeted and efficient ways to treat individual patients. Genomic pathway analyses and other gene-centric investigations have revealed that alterations in the genetic code of integrins and other CAMs, or the proteins mediating CAM signalling, impact on the neural connections and strongly associate with neurodevelopmental disorders, such as ASD (Pinto et al., 2010). In addition, in vitro and in vivo studies have implicated integrins, especially the β1 and β3 integrins, as having a role in the developing nervous system through the regulation of processes associated with neuronal connectivity, such as neurite outgrowth and guidance, formation and maintenance of dendrite spines and synapses and synaptic plasticity (Kerrisk et al., 2014; Park and Goda, 2016). Similarly, in the adult brain, integrins exhibit significant roles in synapse formation and maturation, and furthermore, also regulate synaptic plasticity (McGeachie et al., 2011). In addition, genetic-linkage studies in population cohorts have identified an association between the ITGB3 gene, encoding the human integrin β3-subunit, and ASD (Carter et al., 2011; Lilja and Ivaska, 2018). Indeed, mice lacking *Itgb3* exhibit behavioral abnormalities with a strong analogy to ASD in humans, including abnormal social interactions and repetitive behavior (Carter et al., 2011). In this regard, an ITGB3 missense mutation has been identified in an individual with ASD (O'Roak et al., 2012), further strengthening the role of β3 integrin in autism. Moreover, another study found that a gain-of-function integrin β3 Pro33 variant alters the serotonin system in the mouse brain, leading to elevated whole-blood 5-HT levels and ASD (Dohn et al., 2017). In particular, the integrin β3 Leu33Pro coding polymorphism has been associated with ASD within a subgroup of patients with elevated blood 5-HT

levels, linking integrin β3, 5-HT, and ASD risk. In this study it has been found that the Pro33 coding variation in the murine integrin β3 recapitulates the sex-dependent neurochemical and behavioral attributes of ASD. The presynaptic 5-HT function is altered in these mice, and the localization of 5-HT transporters to specific compartments within the synapse, disrupted by the integrin β3 Pro33 mutation, is critical for appropriate reuptake of 5-HT (Dohn et al., 2017).

Currently, it remains unclear whether β3 integrin contributes to ASD in its capacity as an adhesion receptor and/or as a cytoskeletal regulator, or whether it serves some kind of adhesion-independent scaffolding function that is distinct to those reported in non-neuronal cells (Lilja and Ivaska, 2018).

2.17 Working hypothesis

β3 integrins regulate multiple processes in the developing and mature nervous system such as neuronal connectivity, formation and maintenance of dendritic spines, synapses and synaptic plasticity (Kerrisk et al., 2014) but the molecular mechanisms underlying these functions are still poorly understood. It is plausible that some of these β3 integrin-dependent processes might be because of changes in cytosolic Ca^{2+} influx influenced by activation of SK channels. SK channels are activated by an increase in intracellular Ca^{2+} that enable them to hyperpolarize the membrane potential and to control the neuronal intrinsic excitability. Hence, SK channels control calcium dependent processes through a negative feedback system. The interplay between SK channels and β3 integrin might be important in the developing nervous system, regulating the Ca^{2+} and K^{+} fluxes and consequently the intrinsic excitability of a neuron.

Several studies found that *Itgb3* KO mice are implicated in ASDs. Some ASD-related gene mutations were shown to converge to glutamatergic projection neurons in LV of the

medial-prefrontal cortex (mPFC) around 3-5 postconceptional weeks. In layer V of the mPFC, two different populations of pyramidal neurons -ET and IT- are present. They exhibit different genetic, anatomical and electrophysiological properties; also, ET neurons show alterations in the expression of several ion channels and in neuronal activity in ASD models, while IT neurons do not (Kalmbach et al., 2015; Zhang et al., 2014). It is possible that LV ET *Itgb3* KO neurons have some impairments in intrinsic excitability leading to ASD-like behaviors. To test for impairments in LV pyramidal neuron intrinsic excitability, I characterized the SK-mediated current in LV ET and IT pyramidal neurons in WT and *Itgb3* KO mice and the firing properties of these neurons.

2.18 Aims of the project

Given the above considerations, the overall aim of the thesis is to investigate SK channel-mediated Ca^{2+}-activated K^+ currents in intra- and extra-telencephalic cortical pyramidal neurons of the mPFC in WT and constitutive *Itgb3* KO mice

The specific tasks are:

1) To investigate the SK channel-mediated mI_{AHP} current and the intrinsic excitability of ET and IT pyramidal neurons in WT and *Itgb3* KO mice;
2) To correlate the expression level of β3 integrin and SK2 channels in ET and IT pyramidal neurons with their functional properties.

3 Methods

3.1 Genotyping

All animal procedures were in accordance with the Italian Government and Italian Institute of Technology guidelines for animal welfare used in scientific research. All mice used for experimentation came from two separate colonies of C57BL/6J background. Animals were housed in a temperature- and humidity-controlled room under a 12:12 h light/dark cycle with lights on at 7 am. A constitutive knockout for the gene *Itgb3* was obtained from The Jackson Laboratory (B6.129S2-Itgb3tm1Hyn/J) and was maintained crossing a wild type (*Itgb3*+/+) or a knockout (*Itgb3*-/-) male with heterozygous (*Itgb3*+/-) females. In the former crossing, progeny was composed by 50% Itgb3 WT (*Itgb3*+/+, homozygous wild type) and 50% *Itgb3* Het (*Itgb3*+/-, heterozygous for *Itgb3*), while in the latter crossing, progeny was composed by 50% *Itgb3* KO (*Itgb3*-/-, homozygous knockout) and 50% *Itgb3* Het mice. Although we did not obtain *Itgb3* WT and KO littermates, all mothers had the same genotype (*Itgb3* Het) and were alternated between the two crossing schemes. Thus, WT and *Itgb3* KO mice shared the same mothers. To confirm the genotype of the offspring the DNA was isolated from ear snips or chipped distal phalanges and a standard PCR-based genotyping was performed. All animals were re-genotyped after experimentation. The primer sequences used for PCR genotyping and the size of the PCR products can be seen in **table 1**.

Gene	**Primer sequence**	**PCR Product**
Itgb3	5'-CACGAGACTAGTGAGACGTG-3' 5'-CTTAGACACCTGCTACGGGC-3' 5'-CCTGCCTGAGGCTGAGTG-3'	WT – 4127 bp KO – 533 bp Het – both bands

Table 1. List of primers used for genotyping and their correspondent PCR products.

3.2 Electrophysiological recording

Ex-vivo brain slice preparation: 3 weeks old mice of either sex were drowsed with CO_2 and sacrificed by cervical dislocation. Brains were immediately transferred in an ice-cold dissecting artificial cerebrospinal fluid (aCSF1) containing (in mM): 100 NaCl, 2.5 KCl, 1.25 NaH_2PO_4, 25 $NaHCO_3$, 5 NaAscorbate, 3 NaPyruvate, 25 D-Glucose, 10 $MgSO_4$, 6 NaOH, and 0.5 $CaCl_2$, bubbled with 95% O_2 and 5% CO_2, pH 7.4 and 300 mOsm. Coronal slices (300 µm thick) of the frontal lobe were obtained using a vibratome VT1200 S (Leica) in ice-cold aCSF1. After sectioning, slices were stored for 30 min at 33 °C in the aCSF1, then at room temperature for ≥30 min before being transferred to the recording chamber.

Identification of ET and IT neurons: Tight-seal whole-cell recordings were performed in a submerged chamber at 30 ± 1 ºC with a constant flow (2mL/min) of a recording artificial cerebrospinal fluid 2 (aCSF2) containing (in mM): 120 NaCl, 2.5 KCl, 1.25 NaH_2PO_4, 25 $NaHCO_3$, 12.5 Glucose, 1.5 $MgSO_4$, 6 NaOH, and 2.5 $CaCl_2$, bubbled with 95% O_2 and 5% CO_2, 7.4 pH and 300 mOsm. Glass micropipettes (3 - 5 MΩ) were pulled with a vertical micropipette puller (Narishige) from borosilicate glass capillary tubes (outer dimeter 1.5 mm; inner diameter 1.12 mm, World Precision Instruments) and filled with an internal solution containing (in mM): 110 KGluconate, 20 KCl, 5 NaCl, 10 Hepes, 0.5 EGTA, 1 $MgCl_2$, 4 MgATP, 0.5 NaGTP, 20 Na_2CreatinineP, 7.3 pH and 290 mOsm. All the recordings were obtained from ET and IT layer V pyramidal neurons of the prelimbic and cingulate regions of the medial prefrontal cortex (mPFC) from WT and *Itgb3* KO mice. All the protocols were equally applied to ET and IT neurons in WT and *Itgb3* KO mice. To classify ET and IT neurons a protocol to measure their resonance frequency (R*f*) was applied. To this end, a sinusoidal current was injected with constant amplitude linearly spanning from 1 to 15 Hz in 15 seconds (chirp stimulus) and the

impedance amplitude profile (ZAP) was calculated by the ratio of the fast Fourier transformation product of the voltage response to the fast Fourier transformation product of the stimulus (Dembrow et al., 2010). The resonance frequency is represented as the peak of the ZAP. These recordings were filtered at 2.50 kHz and sampled at 25 kHz.

3.3 Cluster Analysis

2D unsupervised cluster analysis was implemented using the Statistics and Machine Learning Toolbox function, provided by MATLAB. The cluster analysis is implicated in grouping a number of objects into subgroups or "clusters," in a way that objects within each cluster are closer to each other than objects belonging to different clusters. The aim of this analysis is to organize the clusters into a natural hierarchy. This determines successively grouping the clusters themselves so that at each level of the hierarchy clusters within the same group are more similar to each other than those in different groups. Essential to the goals of cluster analysis is the concept of the degree of similarity (or dissimilarity) between the singular objects under clusterization.

Verification of the cluster tree: to verify that the distances (heights) in the tree reflect the original distances accurately, the consistency of the clusters was calculated. The height is represented by the cophenetic distance between the two objects. A way to measure the accuracy of the cluster tree in reflecting the data created by the linkage function is to compare the cophenetic distances with the original distance data generated by the pdist function. If the clustering is valid, the linking of objects in the cluster tree should have a strong correlation with the distances between objects in the distance vector. The cophenetic function compares these two sets of values and computes their correlation, returning a value called the cophenetic correlation coefficient. The closer the value of the cophenetic correlation coefficient is to 1, the more accurately the clustering solution

reflects the data. The cophenetic correlation coefficient calculated for WT neurons was 0.76, for *Itgb3* KO 0.69.

3.4 Isolation and recording of the AHP current in ET and IT neurons

Once the neuron type had been identified, experiments in voltage-clamp configuration were performed to isolate and measure the medium afterhyperpolarization current (mI_{AHP}). Drugs were applied in the bath solution. Voltage clamp recordings were performed in the presence of tetrodotoxin citrate (TTX; 0.5 μM) and tetraethylammonium chloride (TEA; 1 mM) to block voltage-dependent Na^+ channels and TEA-sensitive K^+ channels, respectively. To elicit mI_{AHP}, 100 ms-long depolarizing voltage steps from -40 mV to +100 mV, with intervals of 20 mV steps, are applied from a holding potential of -50 mV. The voltage step selected to record the maximal mI_{AHP} was +40 mV, eliciting an unclamped Ca^{2+} spike and a mI_{AHP} as tail current. A baseline (4 min) was followed by apamin (100 nM) (8 min) application, a high affinity antagonist of SK channels. An agonist of SK channels: 6, 7-dichloro-1H-indole-2,3-dione 3-oxime (NS309 10μM) was applied using the same protocol in the presence of TTX, TEA. NS309 has a positive modulation due to a concentration-dependent increase in the Ca^{2+} sensitivity of the SK channels (Palle Christophersen, 2006). These recordings, performed in voltage-clamp configuration, were filtered at 5 kHz and sampled at 50 kHz.

3.5 Intrinsic excitability of ET and IT neurons

In current-clamp configuration current steps were performed from -160 pA to 300 pA (for IT and to 400 pA for ET neurons), with an increase of 20 pA, before and after the application of apamin (100 nM). Each current step lasted 1000 ms. Afterwards, to understand the relevance of SK channels in the regularity of the cell firing, longer current steps (10 s) from 20 pA to 300 pA for IT and to 400 pA for ET neurons, with an increase

of 20 pA, were applied before and after the application of apamin (100 nM). In current-clamp experiments data were filtered at 5 kHz and sampled at 50 kHz.

Before starting each experiment, the resting membrane potential was measured for all the neurons in current clamp mode, neurons with an initial resting potential ≤ -58 mV were discarded. All protocols included a 100 ms-long hyperpolarizing step of 5 mV to estimate the passive properties of the neurons: input resistance (Rin), access resistance (Rs), membrane capacitance (Cm). Series resistance was monitored at regular intervals throughout the measurement and only recordings with low (≤20MΩ) and stable series resistance were included in this study (≤20% change). No series resistance compensation and no corrections for liquid junction potentials were made. Only cells with a stable resting membrane potential throughout the current-clamp protocols (± 1 mV) were included in the analysis. Data were acquired using a triple patch-clamp EPC10 USB amplifier (HEKA, Lambrecht Germany) and stored on a PC using the Patchmaster (v2 x 73.1) software.

3.6 Electrophysiological analysis

All the analysis was performed by using the following programs: pCLAMP 10 (Axon), Igor Pro 6.03A (Wave Metrics, USA), GraphPad Prism 5.03 and Excel (Micrsoft, USA), MATLAB (Statistics and Machine Learning Toolbox, MathWorks, USA). Results are expressed as mean ± S.E.M. For the experiments in voltage-clamp mode, the amplitude of the mI_{AHP}, the time to peak, the decay time constant and the charge were analyzed using the subtracted trace between the effect of apamin (or of the NS309 when applied) and the baseline. For the experiments in current-clamp mode, the number of action potentials, the spike frequency adaptation and the firing regularity were analysed using pCLAMP 10 (Axon). Coefficients of variation (CVs) were obtained by dividing the

standard deviation by the mean of the interspike intervals. The cluster analysis to group the two neuron types was performed using MATLAB (Statistics and Machine Learning Toolbox, MathWorks, USA). Statistical analysis of two groups of data was performed using Student's *t*-test, with a P-value < 0.05 as significant, when more than two groups were analyzed one-way or two-way analysis of variance (ANOVA) was used with a P-value < 0.05 as significant. A post hoc test (Tuckey Multiple Comparison Test) was used when a significant difference was found in the analysis of variance. All the statistical analysis was performed in GraphPad Prism 5.03 and Excel.

3.7 Intracranial injections

Surgery: WT and *Itgb3* KO mice were used for *in-vivo* injections. AAV retrograde particles (rAAVs) were produced from Synapsin-driven EGFP-expression control: pAAV-hSyn-EGFP (1:5 dilutions in phosphate buffered saline (PBS), Titer: $1.5x10^{13}$ vg/mL, Cat. No. 50465, Addgene). These rAAVs were produced with a retrograde serotype, which permits retrograde access to projection neurons, feature used in this study to label the two different neuron populations. Therefore, the in vivo injections were placed at the projection site of ET and IT neurons: the pontine nuclei (4.16 mm posterior to bregma, 0.4 mm lateral to bregma and 5.65 ventral to bregma) and the contralateral prefrontal cortex (1.98 mm anterior to bregma, 0.4 mm lateral to bregma and 1 mm ventral to bregma) respectively, identified using the Paxinos and Franklin (2001) atlas. Mice were used for the injections at P28. The animal was placed in an induction chamber with an inhalation dose of isoflurane (Isocore 1000mg/g, Isoflurane Vaporizer - Funnel-Fill, Cat.No. 911103, VetEquip) and of oxygen (5 Liter Oxygen Concentrator, Cat. No. 525DS, DeVilbis Healthcare), once deep anesthesia was established, the animal was located in a stereotaxic surgical device (Digital Stereotaxic Frame, Cat. No. 502300,

World Precision Instruments) and supplemental doses of isoflurane and oxygen were given throughout the surgery, as required. At the base of the stereotaxic apparatus was attached a heating blanket (Animal Temperature Controller, Cat. No. ATC-2000, World Precision Instruments) to maintain the body temperature at 37°C throughout the surgery. Once the animal was secured in the stereotaxic apparatus, the surgery started. The eyes were protected by Lacrigel (10g, Dompè) and the head shaved, by using appropriate tools (tweezers and scissors) the skin was cut and the bregma recognized. The distance bregma-interaural was taken to identify the correct site of injection, that was marked and a craniotomy was performed using a drill (HP4-310 Portable Brush type rotary handpiece, Foredom). Borosilicate glass capillary tubes (90 mm in length, outer dimeter 1 mm; inner diameter 0.6 mm, Narishige's GD-1) pulled with a vertical micropipette puller (Narishige), were filled with 1 µL of pAAV-hSyn-EGFP. Using previously calculated X, Y and Z stereotaxic coordinates, the capillary was located over the area to be injected. The injections were manually performed with a 1 ml syringe (BD Luer-Lok Tip) connected to the capillary by an appropriate probe holder for injections. After the injection was finished, the surgical site was rinsed with saline, and the skin sutured. The mouse was left to recover for one night under a IR lamp, the following day transferred in a normal cage provided by the animal facility.

3.8 Immunohistochemistry

Tissue preparation and sectioning: 10/15 days after virus injection, animals were anesthetized with isoflurane (Isocore 1000mg/g) and intracardially perfused, to preserve the morphology of the tissue in a life-like state. At this point the animal was ready to be perfused, 1X PB (10 mL) was injected from the posterior end of the left ventricle using a perfusion needle to the ascending aorta. Finally, an incision to the animal's right atrium

was performed to create an outlet without damaging the descending aorta for drainage. After most of the blood was removed, PB was substituted with 4% paraformaldehyde (PFA; 50 mL) in 1X PB. Once the animal was perfused, the brain was removed and placed into 4% PFA for 6h at 4 °C for postfixation, then transferred in a 30% sucrose solution at 4°C for 24-48h for cryoprotection. Then the brain was frozen in dry ice for 15 minutes, before coronally cutting with a Sliding Microtome (HM 430, ThermoFisher scientific) at thickness of 50 µm and placing into 1X PB at 4°C in order to perform the immunostaining.

Staining for β3 integrins and SK channels: Slices previously cut from fixed pAAV-hSyn-EGFP injected brains were used to stain β3 integrins and SK channels, to analyse their expression in ET and IT neurons. To perform the staining, the Tyramide SuperBoost Kit (Cat. No. B40922 ThermoFisher scientific) with the Alexa Fluor568 Tyramide Reagent (10 min, 1:10 dilution; Cat.No. B40956, ThermoFisher scientific) was used. On the first day slices were washed with Phosphate-Buffered Saline (PBS) (1 X 10 min) and treated for 10 min at 50°C with sodium citrate solution (10 mM tri-sodium citrate dehydrate, pH 6.0, 0.05% Tween-20), to retrieve either the β3 integrin or the SK channel antigen and allow the binding of the antibody. To stop the effect of the antigen retrieval, slices were washed in PBS (4 X 10 min) at room temperature (RT). For quenching endogenous peroxidase, slices were treated with 3% H_2O_2 solution (Cat. No. B40922, Component C2, ThermoFisher scientific) for 30 min at RT. The permeabilization of the antybody in the tissue was enhanced by treating the slices for 30 min at RT with 0.3% TritonX-100. After PBS washes (3 X 10 min) slices were incubated for 1h at RT with 10% normal goat serum (NGS) in PBS (blocking buffer; Cat. No. B40922; Component A, ThermoFisher scientific) to saturate non-specific sites before the application of the antibody. At this stage a primary antibody either for SK channels: rabbit anti-SK2 (1:200; SK2-Rb-Af500d; FRONTIER INSTITUTE Co.Ltd, Hokkaido Japan) or for β3 integrin:

rabbit monoclonal anti-β3 integrin (1:100; Cat. No. 13166, Cell signaling) was diluted in the blocking buffer and incubated with slices overnight/24hrs at 4°C. On the second day of the staining, slices were washed in PBS (4 X 10 min) and incubated for 1h at RT in poly-HRP-conjugated secondary antibody goat anti-rabbit (Cat. No. B40922, Component B, ThermoFisher scientific). After washes in PBS (4 X 10 min), slices were incubated in Tyramide Working Solution (100 X Tyramide stock solution, 100 X H_2O_2 solution and 1 X Reaction buffer; Cat. No. B40922, ThermoFisher scientific). Tyramide was labeled with Alexa Fluor 568 which react with HRP to deposit light and photostable Alexa Fluor orange-red dye on either SK channels or β3 integrins. After, a reaction stop reagent (diluted 1:11 in PBS; Cat. No. B40922, Component D, ThermoFisher scientific) and washes of PBS (4 X 10 min) were performed at RT. As control experiments, a stain for NeuN was performed in parallel. As primary antibody a mouse anti-NeuN was used (1:500, Cat. No. MAB377 Millipore), as secondary antibody a goat anti-mouse Alexa Fluor568 (1:500, Cat. No. A-11004, ThermoFisher scientific).

Enhancement of EGFP signal: Once the staining for SK channels or β3 integrins was completed, a stain to boost the signal of the EGFP previously injected in the two neuron types was performed. Prior the application of the antibody, slices were treated for 30 min at RT with 10% PBS-NGS, after incubated for 2h at RT with a primary antibody chicken anti-GFP (1:1000; Cat. No. 135304, Synaptic System) diluted in the blocking buffer. Washes in PBS (4 X 10 min) were performed and slices incubated for 1h at RT with a secondary antibody goat anti-chicken Alexa Fluor488-conjugated. Finally, washes with PBS (4 X 10 min) were performed and the slices transferred on slides, when dried mounted with ProLong Gold Antifade Mountant (Cat. No. P36934, ThermoFisher scientific) and left in the dark and on a flat surface to dry overnight. All the experiments were performed avoiding direct light on slices since injected with EGFP. From one brain,

three slices were used to stain β3 integrins and other three to stain SK channels. In total, to perform these experiments three mice WTET, three *Itgb3* KOET, three WTIT and three *Itgb3* KOIT were used.

3.9 Confocal microscopy and image analysis

When the slides were dry, confocal stacks were acquired with a Leica SP8 using a 40x oil immersion objective (NA 1.40), with one µm between optical sections, a sequential line-scan mode and 3x scan averaging. For all experimental conditions compared, the same settings for laser intensity, offset and PMT gain were used. Confocal images were analysed using ImageJ. The maximal fluorescence intensities of in-focus stacks were Z-projected and the resulting images were automatically thresholded using the Robust Automatic Threshold Selection plugin. Regions of interests (ROIs) were manually drawn around the soma of layer V retrogradely labeled neurons in the green channel (> 10 neurons/section) and fluorescence intensity was measured in the red channel. The fluorescence intensity values for all neurons on the slice were then averaged. For each staining, the quantification was performed on three slices per injected animal, in total three animals were injected per neuron type and genotype.

3.10 Statistical Analysis

Statistical analysis was performed with paired or unpaired Student's t-test, or with One- or Two-way analysis of variance (ANOVA) and Tukey's multiple comparisons test, using Prism GraphPad, as indicated. Box plots show the mean. Dots represent individual samples. Data in bar charts and line graphs are shown as mean ± standard error of the mean (sem).

4 Results

4.1 Cluster analysis of ET and IT neurons in WT and *Itgb3* KO neurons

Mice lacking *Itgb3* gene exhibit behavioral anomalies with a strong analogy to ASD in humans, including abnormal social interactions and repetitive behavior (Carter et al., 2011; Lilja and Ivaska, 2018; O'Roak et al., 2012), on the other hand ET layer V pyramidal neurons of the mPFC have been described to be more prone to develop ASD-related mutations during the development (Willsey et al., 2013), than IT neurons. Since our lab has found a protein-protein interaction between β3 integrin and SK channels (unpublished data), both intensely expressed at layer V of mPFC, the purpose of my thesis is to characterize this interaction from the physiological point of view, to shade new light on the role of β3 integrin in ASD. In order to identify ET and IT neurons at layer V of the mPFC an agglomerative hierarchical cluster analysis was performed. The neuronal classification was implemented by using two passive neuronal properties the Rf and the R_{in}, as showed from a previous study (Dembrow et al., 2010). The results of the cluster analysis are reported in the **(Fig.1).** The cophenetic correlation coefficient (an indicator for the quality of the cluster) was higher for WT neurons (0.76) **(Fig.1A**), then *Itgb3* KO neurons (0.69) **(Fig.1B)**. This means that WT, ET and IT were better divided than *Itgb3* KO, ET and IT. The same trend is reported by the **(Fig.1C, D)** where a scatter plot with marginal histograms is shown. In the **(Fig.1C),** the two clusters for WT neurons were well separated**,** while for *Itgb3* KO mice the two clusters were similar **(Fig.1D)**. Rf and R_{in} were significantly different between ET and IT neurons (Rf ET-IT $p<0.001$; R_{in} ET-IT $p<0.001$), while no significant differences were found between the two genotypes. The cluster analysis identified all ET neurons with a Rf above 2 Hz, and all IT neurons with a

Rf below 2 Hz, except for three neurons, namely 2 WT (Rf = 2.65432 Hz and 2.10156 Hz) and 1 *Itgb3* KO (Rf = 2.07247 Hz) neuron with a Rf just above 2 Hz. These neurons were classified as ET neurons, since other passive properties were closer to ET than IT neurons. Previous studies performed in rats (Dembrow et al., 2010) (Dembrow et al., 2015) and the present performed in mice, confirm the presence of two different neuron types in the layer V of mPFC characterized by their differences in Rf and the R_{in}. The differences found in all the passive and active properties (see below) and in the cluster analysis make a strong statement of the individuality of these two neuron-types.

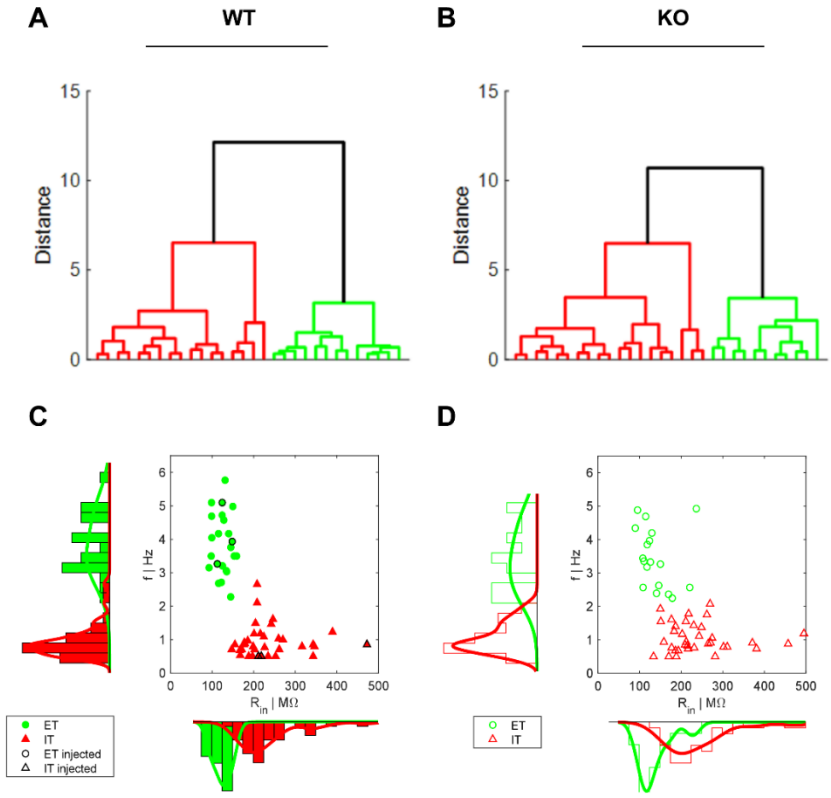

Fig.1 Agglomerative hierarchical cluster analysis. (A, B) Dendrograms from hierarchical cluster analysis, for WT **(A)** and *Itgb3* KO **(B)** neurons. In the figure, the horizontal axis represent the indices of the objects in the original data set. The links between objects are represented as upside-down U-shaped lines. The height of the U indicates the distance between the objects. **(C, D)** Scatter plot from cluster analysis, Rf is plotted against R_{in} for WT **(C)** and *Itgb3* KO **(D)** neurons. In the scatter plot WT there are 3 ET and 3 IT, which are labeled with black borders, identified via retrograde labelling (details below). (nWT=55, nKO=53. Rf ET-IT $p<0.001$, R_{in} ET-IT $p<0.001$. Two-way ANOVA)

4.2 Resonance frequency: a way to recognize ET and IT neurons in the mPFC

The resonance frequency has been used as a tool to identify ET and IT neurons. The resonance is a property that describes the frequency at which a neuron elicits the maximal voltage response to sinusoidal current injections of different frequencies (Hutcheon and Yarom, 2000). Individual neurons can have frequency preferences determined by the expression of different voltage-gated conductances, in particular by the presence of the hyperpolarization-activated *h* and M-type K^+ conductances (Dembrow et al., 2010). The membrane voltage will resonate with inputs of a specific frequency, while filtering out inputs at other frequency acting as bandpass (ET neurons) and low-pass filters (IT neurons) (Dembrow et al., 2010). These two neuron types were characterized by different dynamic and steady-state intrinsic properties (see below). To validate subthreshold dynamic properties such as Rf and resting membrane potential (Vm) a sinusoidal current with constant amplitude linearly increased in frequency (chirp stimulus) was injected into the soma **(Fig.2A)**. ET neurons showed membrane resonance after the chirp stimulus **(Fig.2B)** while IT neurons were not resonant (**Fig.2C)**. The resonance frequency, ***Rf*** varied from 0.5 Hz to 6 Hz.

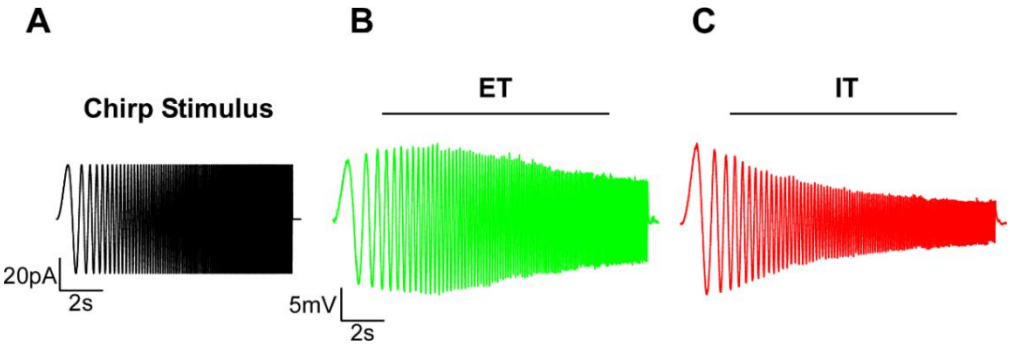

Fig.2 Resonance frequency (Rf) (A) A chirp stimulus with increasing frequency from 1 to 15 Hz in 15 s. The amplitude of the chirp stimulus used was 60 pA, **(B)** Example traces of resonant ET neurons and **(C)** non-resonant IT neurons.

4.3 Passive and active properties of ET and IT neurons in WT and *Itgb3* KO neurons

In order to characterize the physiology of ET and IT neuron types in WT and *Itgb3* KO neurons, their passive and active properties were analyzed. In previous studies, these two neuron types were shown to exhibit different passive and active properties, although at morphological level, there were no differences in the size and shape of the soma (Christophe et al., 2005; Dembrow et al., 2010). In **Table1** are reported all the properties described in this study. In general, between ET and IT neurons there were significant differences in all the passive and active properties considered, aside from the access resistance that is indicative of the opening state of the cell during the experiment. In particular, the Vm was more depolarized in ET than IT neurons, the R_{in} and the Cm were higher in IT than ET, while the fR was higher in ET than IT neurons. For all the conditions, no significant differences were found between the two genotypes, apart from the Cm that is proportional to the membrane surface. The Cm was the only passive property that significantly changed ($p=0.03$) between the WT and *Itgb3* KO ET neurons. For the purpose of this study only one active property, the rheobase, was analysed since it was already described to be different between these two neuron types (Dembrow et al., 2010). The rheobase was higher in ET than IT neuron types, this is also evident from the **(Fig.6C)** where ET neurons require more current to fire the first action potential than IT **Table1**. These results show a consistent diversity (statistical values are reported in the figure legend of **Table1**) of the two neuron types ET and IT in all the passive and active properties considered, which is in line with previous reports (Dembrow et al., 2010; Shepherd, 2013). On the other side, no consistent differences were observed for the two genotypes, WT versus *Itgb3* KO ET and WT versus *Itgb3* KO IT. Only the C_m was statistical different between WT and *Itgb3* KO ET neurons (statistical values are reported

in the figure legend of **Table1**), it might be possible that *Itgb3* KO ET neurons have some impairment of the membrane surface since their C_m is higher when compared to the WT ET neurons.

	WT ET	KO ET	WT IT	KO IT
V_m (mV)	**-66 ±0.6**	**-65±0.6**	**-70±0.7**	**-70±0.7**
R_{in} (MΩ)	**132.56±5.9**	**145.0±11.3**	**229.68±11.5**	**240.17±14.3**
Rf (Hz)	**3.74±0.1**	**3.38±0.2**	**0.87±0**	**1.03±0**
Rs (MΩ)	**13.91±0.5**	**14.19±0.9**	**13.91±0.5**	**13.82±0.4**
Cm (pF)	**277±11.9**	**327±20**	**405±18.2**	**395±15.1**
Rheobase (pA)	**200±13.5**	**192±13.2**	**140±9.7**	**141±10.9**
n	**25**	**19**	**30**	**34**

Table1. Passive and active properties of ET and IT neurons. All the neurons were analysed for the following passive properties: Vm, R_{in}, Rf, Rs, C_m and active property: rheobase. (Vm ET-IT $p<0.001$, R_{in} ET-IT $p<0.001$, Rf ET-IT $p<0.001$, C_m ET-IT $p<0.001$, C_m WTET-KOET $p=0.03$, rheobase ET-IT $p<0.001$ Unpaired t-Test.). Data are displayed as mean ± SEM.

4.4 Isolation of the medium afterhyperpolarization current

Previous data from my laboratory revealed expression of β3 integrin in layer V pyramidal neurons of the mPFC as revealed by immunostaining and a biochemical interaction between β3 integrin and SK channels (unpublished data), also expressed in the same neurons (Sailer et al., 2004). I therefore addressed whether β3 integrin affected mI_{AHP} and intrinsic excitability of ET and IT layer V pyramidal neurons. SK channels are responsible for the mI_{AHP}, thus in order to isolate this current, experiments in voltage clamp configuration were performed. To identify the current that underlies the mAHP, 100 ms-long depolarizing voltage steps were applied from the holding potential of -50 mV from -40 mV to 100 mV, every 30 s in the presence of tetrodotoxin (TTX; 0.5 µM) to block

voltage-gated Na^+ channels and tetraethylammonium chloride (TEA; 1 mM) to block K^+ channels, in particular BK channels. Under these conditions, it was possible to trigger a Ca^{2+} influx through voltage-gated Ca^{2+} channels and record the mI_{AHP} as tail currents following the Ca^{2+} entry. To validate that the tail current elicited was SK channel-dependent, the antagonist apamin (100 nM) was applied. Apamin is a specific antagonist of SK channels (Wang et al., 2015), has very high affinity for SK channels and may inhibit them by acting as an allosteric inhibitor (Lamy et al., 2010). Apamin eliminated the tail current in both neuron types indicating SK channels as major channels responsible for mI_{AHP} under these recording conditions. The current/voltage (I-V) curve **(Fig.3)** was used to identify the most suitable voltage at which the mI_{AHP} was elicited. The voltage was selected at +40 mV. In particular, a 100 ms-long pulse to 40 mV was used to elicit the apamin-sensitive AHP current (I_{AHP}).

The mI_{AHP} significantly increased from 0mV to 100mV depolarizing voltage steps in ET when compared to IT neurons **(Fig.3)**. Between genotypes, a more significantly increased current in WT than *Itgb3* KO ET neurons was observed only at 20mV, while from 0mV to 100mV the mI_{AHP} was significantly smaller in WT than *Itgb3* KO IT neurons (statistical values are reported in the figure legend of **Fig.3**)

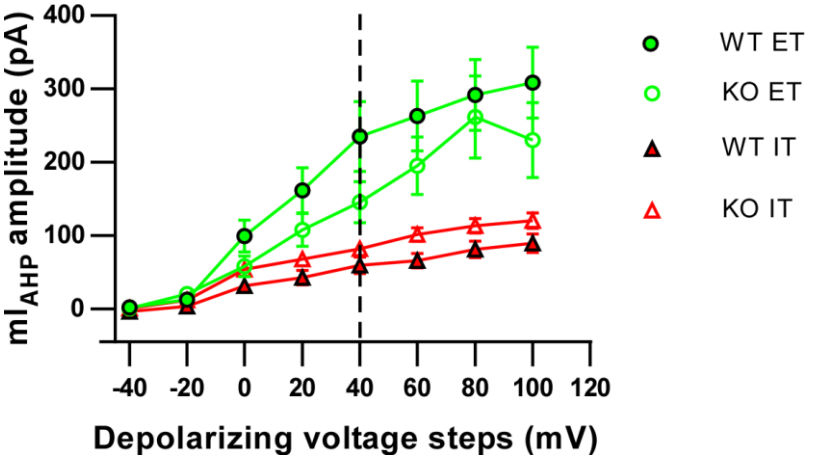

Fig.3 I-V curve. To isolate the medium afterhyperpolarization current (mI_{AHP}) depolarizing voltage steps form -40 mV to 100 mV for 100 ms, were applied. Statistical differences are observed at 0 mV between WTET and WTIT, at 20 mV between WTET and WTIT, and between KOET and WTIT and at 40, 60, 80 and 100 mV between WTET and WTIT, KOET and WTIT and between WTET and KOIT. (nWT ET=10; nKO ET=8; nWT IT=10 nKO IT=14. At -20mV WTIT-KOIT p=0.008. At 0mV WTET-WTIT p=0.04, WTIT-KOIT p=0.02. At 20mV WTET-KOET p=0.02, WTET-WTIT p=0.01, WTIT-KOIT p=0.006. At 40mV WTET-WTIT p=0.02, WTIT-KOIT p=0.03. At 60mV WTET-WTIT p=0.01, WTIT-KOIT p=0.01. At 80mV WTET-WTIT p=0.01, WTIT-KOIT p=0.03. At 100mV WTET-WTIT p=0.008, WTIT-KOIT p=0.03. Two-way ANOVA, Tukey's multiple comparisons test). Data are displayed as mean ± SEM.

4.5 Analysis of medium afterhyperpolarization current

In order to analyse the pharmacological and kinetic features of the mI_{AHP}, a depolarizing voltage step at +40 mV for 100 ms was applied in the presence of TTX, TEA and apamin for both neuron types and genotypes. This depolarization leads to the activation of Ca^{2+} channels, fundamental for the subsequent opening of SK channels. Upon repolarization, the activity of SK channels was recorded as a tail current **(Fig.4)** and inhibited when apamin was added **(Fig.4A)** (Apamin). The analysis was performed on the subtracted traces before and after application of apamin **(Fig.4A)** (Subtracted) **(Fig.4A, B)**. Considering the two neuron types the mI_{AHP} was significantly bigger in ET than IT neurons. For the genotypes the situation was different, the mI_{AHP} was significantly bigger

in WT ET when compared to *Itgb3* KO ET neurons, while very similar in WT IT and *Itgb3* KO IT **(Fig.4C)**.

For a better characterization of mI_{AHP}, I next analyzed the kinetics of this current. One of the properties analysed was the time of peak of mI_{AHP}, because it might be indicative of the distance between SK channels and the Ca^{2+} source. There are significant differences for the time of peak of mI_{AHP} only between ET and IT neurons, possibly suggesting that Ca^{2+} sources are closer to SK channels in ET than IT, inducing a faster current in ET than IT neurons. Instead, there were not significant differences considering the two genotypes for ET and IT neurons (WT and *Itgb3* KO) **(Fig.4B, D)**. The time of peak describes the time at which SK channels are maximally opened; in ET neurons this occurs earlier (~ 14 ms) than in IT neurons, suggesting that SK channels are either closer to the Ca^{2+} sources than IT neurons or that ET neurons have lower Ca^{2+} buffering capacity than IT neurons, as previously reported (Christophe et al., 2005).

The decay time constant of mI_{AHP} is ~ 100 ms (Pedarzani et al., 2005). It represents the elapsed time required for the system to decay back to baseline values, the longer the decay time constant the more the $[Ca^{2+}]_i$ available to activate the SK channels. There are not significant differences between ET and IT neurons and between the two genotypes **(Fig.4B, E)**. In general, these results indicates that, in WT, ET neurons have a larger mI_{AHP} than IT neurons and that, within ET neurons, mI_{AHP} is larger in WT than *Itgb3* KO.

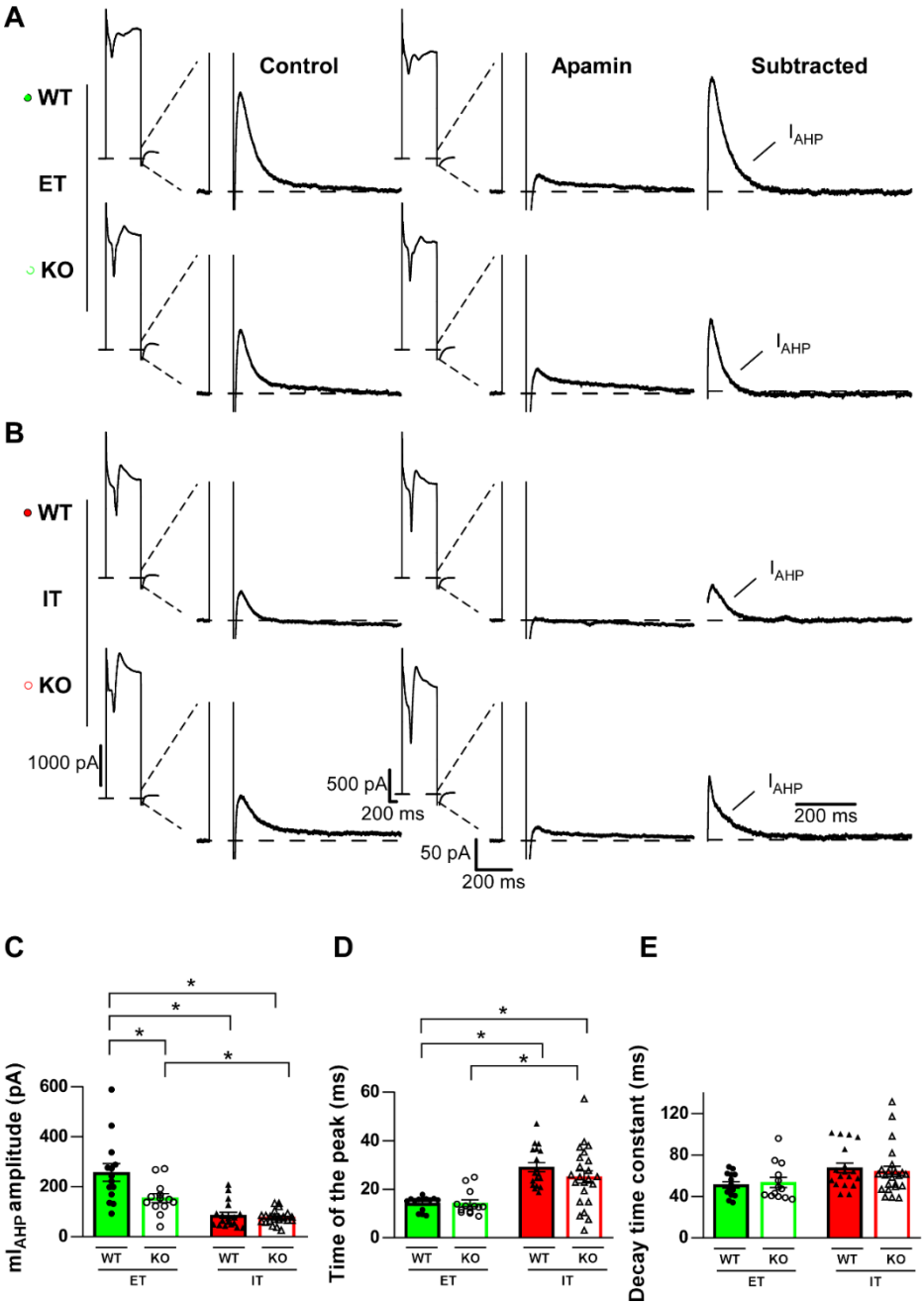

Fig.4 Analysis of SK-mediated mI_{AHP}. (A, B) mI_{AHP} as control (left) and with presence of apamin (100 nM) (middle), in the right panel is shown the subtraction between control and apamin, to isolate the SK-mediated current. The traces reported are for WT and *Itgb3* KO ET **(A)** and IT **(B)** neurons. **(C-E)** Bar diagrams show the amplitude **(C)**, the time to peak **(D)** and the decay time constant **(E)** of ET and IT neurons in WT and *Itgb3* KO mice. The values were calculated on the subtracted trace between the control and the application of apamin. (nWT ET=14; nKO ET=13; nWT IT=18 nKO IT=23; mI_{AHP} amplitude WTET-KOET p=0.002, WTET-WTIT p<0.0001, WTET-KOIT p<0.0001, KOET-KOIT p=0.01; time of the peak WTET-WTIT p<0.0001, WTET-KOIT p=0.002, KOET-WTIT p<0.0001, KOET-KOIT p=0.003. One-way ANOVA, Tukey's multiple comparisons test). Data are displayed as mean ± SEM.

To understand the diversity of the $mI_{AHP,}$ found in the previous experiments, a chemical compound that enhanced the activity of SK channels, the 6,7-dichloro-1H-indole-2,3-dione3-oxime (NS309; 10 µM) (Pedarzani et al., 2005; Shepherd, 2013) was used.

NS309 enhances the activity of SK channels in the presence of intracellular calcium, by increasing the SK sensitivity to Ca^{2+}. To test the effect of NS309 on the kinetics of SK current the same protocol was used as for testing the effect of apamin. For these experiments, NS309 was applied for several minutes (16.15 min) to reach a maximal and stable enhancement of the mI_{AHP} as shown from the time course in **(Fig.5C)**. The data were calculated on the traces from which the effect of the apamin was subtracted **(Fig.5A, B)** (Subtracted). Application of NS309 increased the charge transfer, the decay time constant and, to a smaller extent, the amplitude of the $mI_{AHP,}$ for all the conditions. However, no statistical difference was found. This could be due to the little number of repetitions, at least for WT (4 cells) and *Itgb3* KO (5 cells) ET neurons. The values reported in the **(Fig.5D-F)** are shown as percentage of NS309 effect on the mI_{AHP} amplitude, the decay time constant and the charge transfer. In **(Fig.5D)** the percentage of mI_{AHP} amplitude, of the decay time constant and of the mI_{AHP} charge transfer is quite similar in all the conditions. In general, the presence of NS309 is not changing the mI_{AHP} amplitude in WT ET neurons, while increasing it in all the other conditions **(Fig.5D)**. The decay time constant was increased for all the conditions **(Fig.5E)** and **(Fig.5A** and **B)** (Subtracted), with no differences among all the neurons. The strongest effects were found for mI_{AHP} charge transfer **(Fig.5F** and **Fig.5A** and **B)** (Subtracted), although with no differences for all the conditions. In particular, to better understand the behavior of WT and *Itgb3* KO ET neurons more experiments are needed, while for WT and *Itgb3* KO IT neurons no differences in the effect of the NS309 were found, despite a general increase for all the kinetic properties. All the neurons responded in the same way to NS309, with

a clear increase of the decay time constant, of the charge transfer and a little of the mI_{AHP} amplitude.

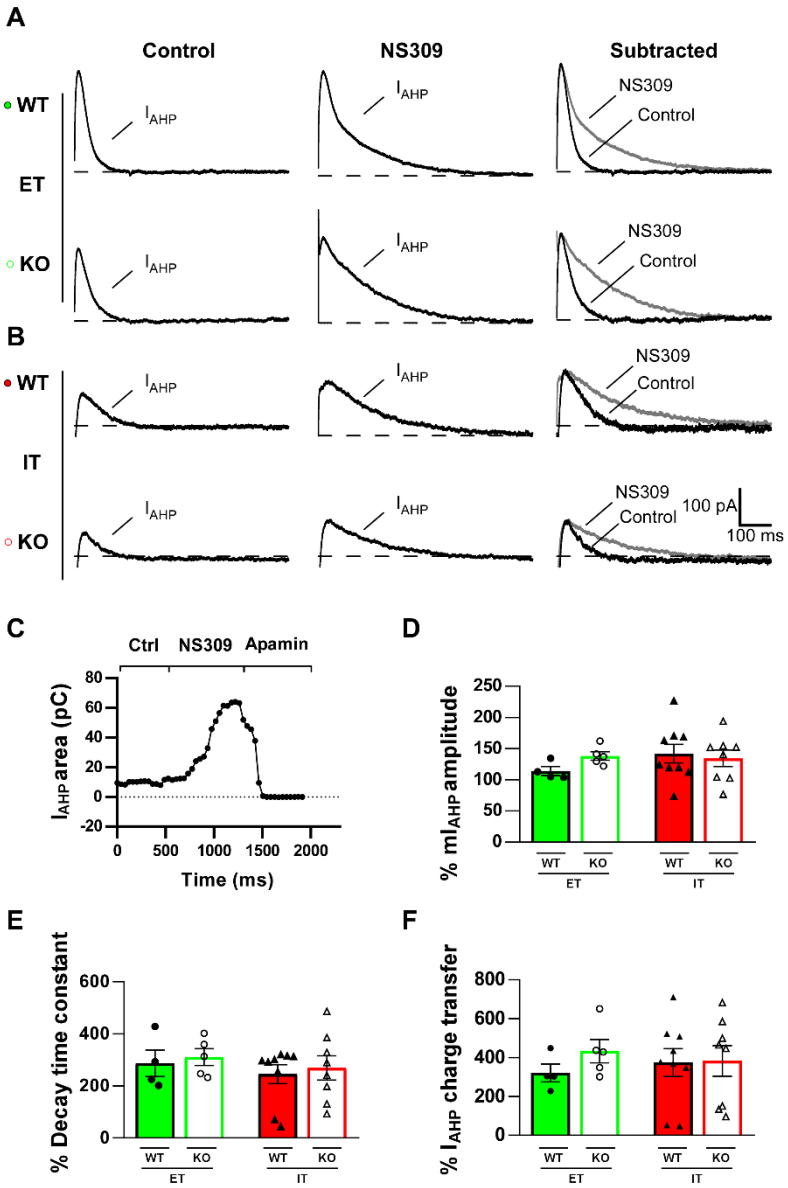

Fig.5 Effect of NS309 on SK-mediated mI_{AHP}. (A, B) mI_{AHP} as control (left), with presence of NS309 (10 µM) (middle), and as subtraction between control and apamin (100 nM) (right), the gray is the normalization of the NS309 effect on the apamin subtracted control for WT and *Itgb3* KO ET **(A)** and IT **(B)** neurons. **(C)** Time course of action of NS309 (10 µM) on the mI_{AHP} shown as charge. mI_{AHP} was elicited every 30 s. NS309 was followed by application of apamin which completely blocked the enhanced effect of NS309. **(D, E, F)** Effect of NS309 in percentage on the charge transfer **(D)**, on the decay time constant **(E)** and on the amplitude **(F)**. (nWT ET=4; nKO ET=5; nWT IT=9 nKO IT=8; One-way ANOVA, Tukey's multiple comparisons test). Data are displayed as mean ± SEM.

4.6 Firing properties of ET and IT in WT and *Itgb3* KO mice

In many pyramidal neurons, action potentials are followed by a prominent afterhyperpolarization (AHP), mediated also by the activation of different types of Ca^{2+}-activated K^+ channels. In particular, the SK channels are responsible for the mAHP in many neuronal types; they regulate the firing pattern and the spike frequency adaptation in neurons (Adelman et al., 2012; Stocker, 2004). To characterize the firing properties of ET and IT neurons in WT and *Itgb3* KO mice, 1-s long depolarizing current steps were applied form -160 pA to 300 pA for IT and to 400 pA for ET neurons with a step of 20 pA between each current step **(Fig.6),** in both genotypes. The recordings were always performed before and after application of apamin (100 nM). ET neurons needed more current to fire the first action potential compared to IT in WT and *Itgb3* KO neurons **(Fig.6).** The action potentials are plotted before and after the application of apamin for the two neuron types ET and IT and for the relative genotype *Itgb3* KO ET and IT neurons **(Fig.6C-D)**. In the control **(Fig.6C)**, there are no differences in the number of action potentials between the two neuron types. Interestingly, during the last current injections, there is a significant difference of action potentials between WT and *Itgb3* KO ET neurons, which is reduced when apamin is applied **(Fig.6D)**, suggesting to be SK-dependent. This means that in ET neurons the firing is β3 integrin dependent, at high depolarizing voltage steps. When apamin is applied **(Fig.6D)**, this difference in the firing between WT and *Itgb3* KO ET neurons disappears. This is due to a significant increase of the firing for WT ET neurons ($p=0.01$), while for *Itgb3* KO ET the increase was not significant. This means that the firing of ET neurons depend on both β3 integrin and SK channels. Indeed, the loss of β3 integrin makes the firing SK-independent, probably because when β3 integrin is missing the SK channels are not properly functioning, therefore the presence of apamin does not have a significant effect on *Itgb3* KO ET

neurons. For ET neurons, the firing is dependent on the complex β3 integrin-SK channels. For IT neurons is dependent only on SK channels. Overall, the presence of apamin significantly increased the firing for ET (p=0.01) and IT (p=0.01) neurons, for the *Itgb3* KO counterparts ET and IT the firing was not significantly increased.

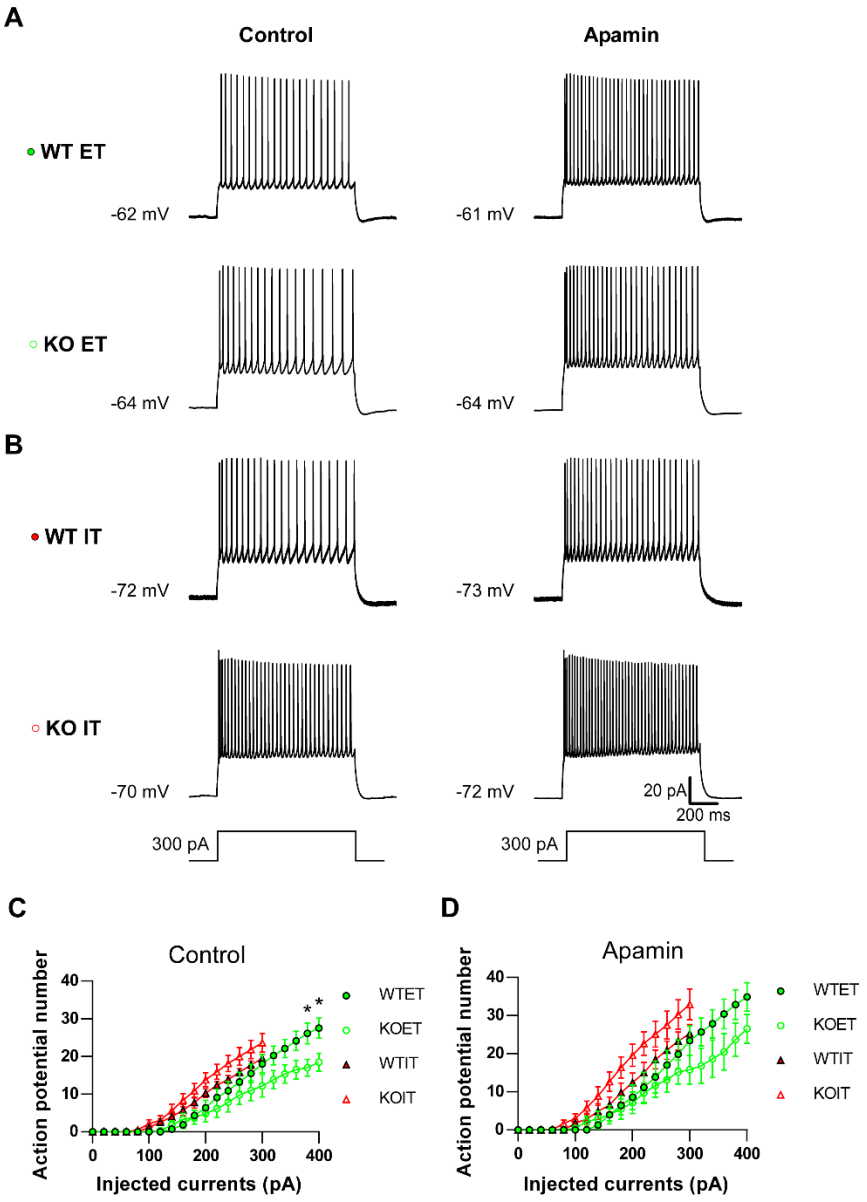

Fig.6 Firing patterns of WT and *Itgb3* KO ET, WT and KO IT neurons. (A, B) Responses to 1s-long depolarizing current injection (300 pA) for all the conditions, in control (left) and with presence of apamin (right). **(C, D)** The number of action potential is plotted versus the injected currents for all the conditions, in control **(C)** and with presence of apamin **(D)**. (For control: nWTET=8; nKOET=6; nWTIT=10; nKOIT=11. For apamin: nWTET=7; nKOET=6; nWTIT=9; nKOIT=10. WTET-KOET: * p=0.02, unpaired t-Test.). Data are displayed as mean ± SEM.

4.7 The role of SK channels in spike frequency adaptation (SFA) and firing precision of WT and *Itgb3* KO ET and IT neurons

In order to investigate the function of SK channels in the spike frequency adaptation of the two neuron types in WT and *Itgb3* KO neurons the frequency of action potentials was analysed during the application of 1-s long depolarizing current step at 300 pA, in control and with application of apamin **(Fig.7A-D)**. In the **(Fig.7A)** is reported the interspike frequency plotted against the time of the response to 1-s long depolarizing step at 300 pA, at t=0 is plotted the first interspike frequency. The interspike frequency is higher for IT than ET neurons, the same trend is evident in *Itgb3* KO IT and ET neurons. With the presence of apamin **(Fig.7B)** there is a general increase in the interspike frequency for all conditions, although with no significant differences. This is expected, because SK2 channels are reported to be implicated in the regulation of the firing patterns, controlling the spike frequency adaptation (Adelman et al., 2012; Stocker, 2004). To analyse the SFA the following formula was used: (Interspike frequency of the first action potential (F1)-the interspike frequency of the last interspike frequency (Flast))/Interspike frequency of the first action potential (F1). As for the interspike frequency, the SFA was calculated from the response to 1-s long depolarizing step at 300 pA **(Fig.7C-D)**. In accordance with the literature (Dembrow et al., 2010), in the control **(Fig.7C)**, there is a significant increase of the adaptation in IT neurons when compared to ET, moreover there are not significant differences when the two genotypes are compared. Interestingly, when apamin is applied ET neurons show a significant increase of the adaptation compared to IT neurons **(Fig.7D)**. It is possible that in ET neurons, as also suggested from the **(Fig.4 A, D)**, the Ca^{2+} sources are closer to SK channels, therefore SK channels are rapidly activated by the first APs showing less adaptation, that increases with the presence of apamin. In IT neurons a different behavior is observed, in control conditions these neuros adapt more

than ET, as described in the literature (Dembrow et al., 2010), whereas with the presence of apamin there is no effect. As consequence, SK channels are responsible for the adaptation only in ET neurons, no implication of SK channels is noticed for the adaptation of IT neurons. These results show an increased adaptation for IT neurons in control condition that is reduced when apamin is applied, on the other side for ET neurons there is a reduced adaptation in control condition, which is significantly increased with application of apamin. Thus, the SFA is SK-dependent in ET neurons, but not in IT neurons. Between WTs and *Itgb3* KOs there were not differences, meaning that the absence of interaction β3 integrin-SK channels is not determinant for the SFA in neither neuron types.

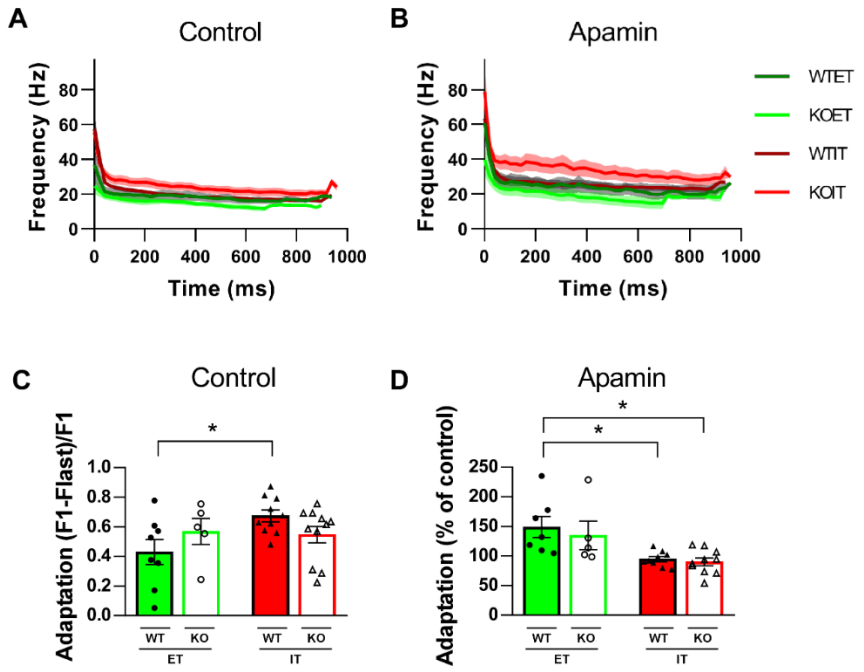

Fig.7 Interspike frequency and SFA. (A, B) The interspike frequency is plotted against the time (1s-long) of the depolarizing current injection at 300 pA for all the neurons, in control **(A)** and with presence of apamin **(B)**. **(C, D)** The spike frequency adaptation is calculated at 300 pA depolarizing current step response for all neurons **(C)**. The % of adaptation is reported related to the control, **(D)**. (For control: nWTET=8; nKOET=6; nWTIT=10; nKOIT=11. For apamin: nWTET=7; nKOET=6; nWTIT=9; nKOIT=10. Control WTET-WTIT p=0.04; apamin WTET-WTIT p=0.001, WTET-KOIT p=0.007 Ordinary One-way ANOVA Tukey's multiple comparisons test). Data are displayed as mean ± SEM.

Further, to assess the role of SK channels in the precision of the firing for both neuron types and genotypes the coefficient of variation (CV) was analysed after 10-s long depolarizing current step at 300 pA **(Fig.8A-D)**. The CV was calculated from the lasts 9s to avoid the first 1s where the phenomenon of the adaptation is occurring. In the control, **(Fig.8 A, B left and C)** WT ET neurons have a very low CV value compared to the *Itgb3* KO, where there are two cells with a high variation. For WT and *Itgb3* KO IT neurons, the CV is low and similar to WT ET neurons. No differences between genotypes were found. In the presence of apamin **(Fig.8 A, B right and D)** WT and *Itgb3* KO ET and *Itgb3* KO IT didn't show changes in their variability, only WT IT neurons increased their CV, although with not significance when compared to WT ET neurons or *Itgb3* KO IT. From these data it is possible to suppose that in ET neurons the firing precision is not SK-dependent, while it could be for IT neurons.

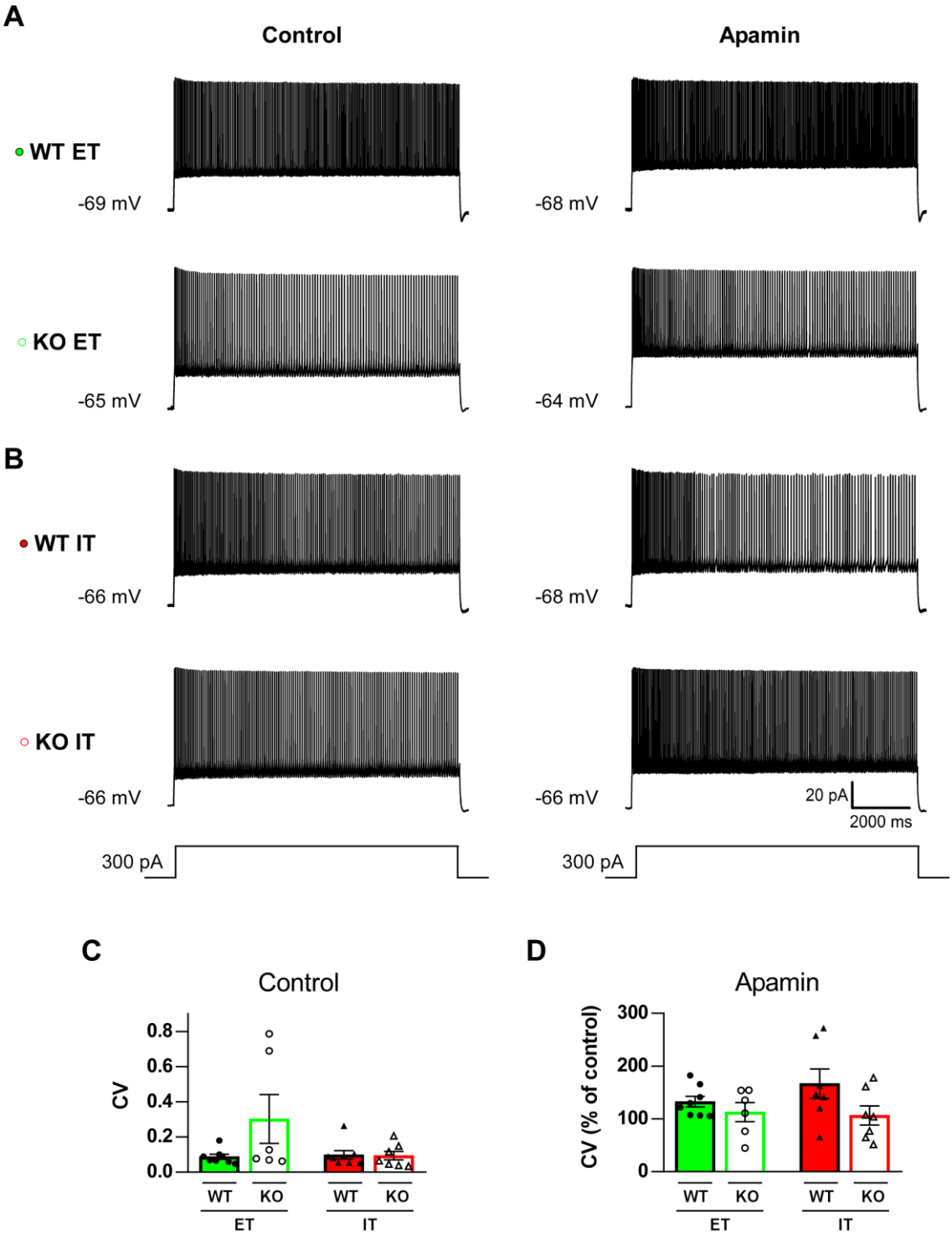

Fig.8 Coefficient of variation (CV). (A, B) Responses to 10s-long depolarizing current injection at 300 pA for all the conditions, in control (left) and with presence of apamin (right). **(C, D)** The CV is calculated at 300 pA depolarizing current step response for all neurons **(C)**. The CV is reported related to the control, a value above 100% was more variable than the control, below not **(D)**. (For control: nWTET=8; nKOET=6; nWTIT=8; nKOIT=7. For apamin: nWTET=8; nKOET=6; nWTIT=7; nKOIT= 7. Ordinary One-way ANOVA Tukey's multiple comparisons test). Data are displayed as mean ± SEM.

4.8 Immunostaining for SK channels and β3 integrin

These experiments were conducted in collaboration with Dr F. Jaudon. To further understand the differences found between the ET and IT and between the WT and *Itgb3* KO an immunostaining was performed for SK channels and β3 integrin in the layer V of the mPFC **(Fig.9 A-E)**. To this end, WT and *Itgb3* KO ET and IT neurons were first labelled *in vivo* by injection with a retrograde AAV into the pons or the controlateral side, respectively, to allow expression of an enhanced green fluorescence protein (EGFP), only ET and IT neurons in the layer V mPFC for all conditions. After 10-14 days of expression, brains were fixed and immunostaining for SK2 and β3 integrin performed on slices (see methods). In **(fig.9A)** (left) GFP fluorescence is shown in green for ET or IT neurons, while SK channel are in red. In the merge, it is possible to see the different expression of SK channels in the two neuron types, in the top merge (IT) the majority of neurons are either red or green, only in a few there is the overlap between green and red meaning that SK channels can be found only in some IT neurons. Further, SK2 mean fluorescence intensity is reduced in IT when compared to ET neurons **(Fig.9C)**. In the merge for ET WT **(Fig.9A)** there is more overlap of green and red fluorescence, meaning greater expression of SK channels in ET neurons **(Fig.9C)**. Equivalently, there are more SK channels in *Itgb3* KO ET than in *Itgb3* KO IT neurons **(Fig 9B, C)**. In the **(fig.9A)** (middle), the green fluorescence is marking the two neuron types and the red fluorescence is targeting the β3 integrin. The merge and the **(Fig.9D)** indicates the same level of β3 integrin in ET and IT neurons. In the last panel of the **(Fig.9A)** NeuN in red, used as a marker for all neurons. The merged panels in A-B (right) and **(Fig.9E)** show the same level of NeuN expression for all the conditions, as expected. These results indicate an increased SK channels expression in ET than IT neurons, irrespective of the genotype.

Moreover, the level of β3 integrin was very close in the two neuron types. Taken together, these founding are in line with the different mI_{AHP} found in voltage clamp experiments.

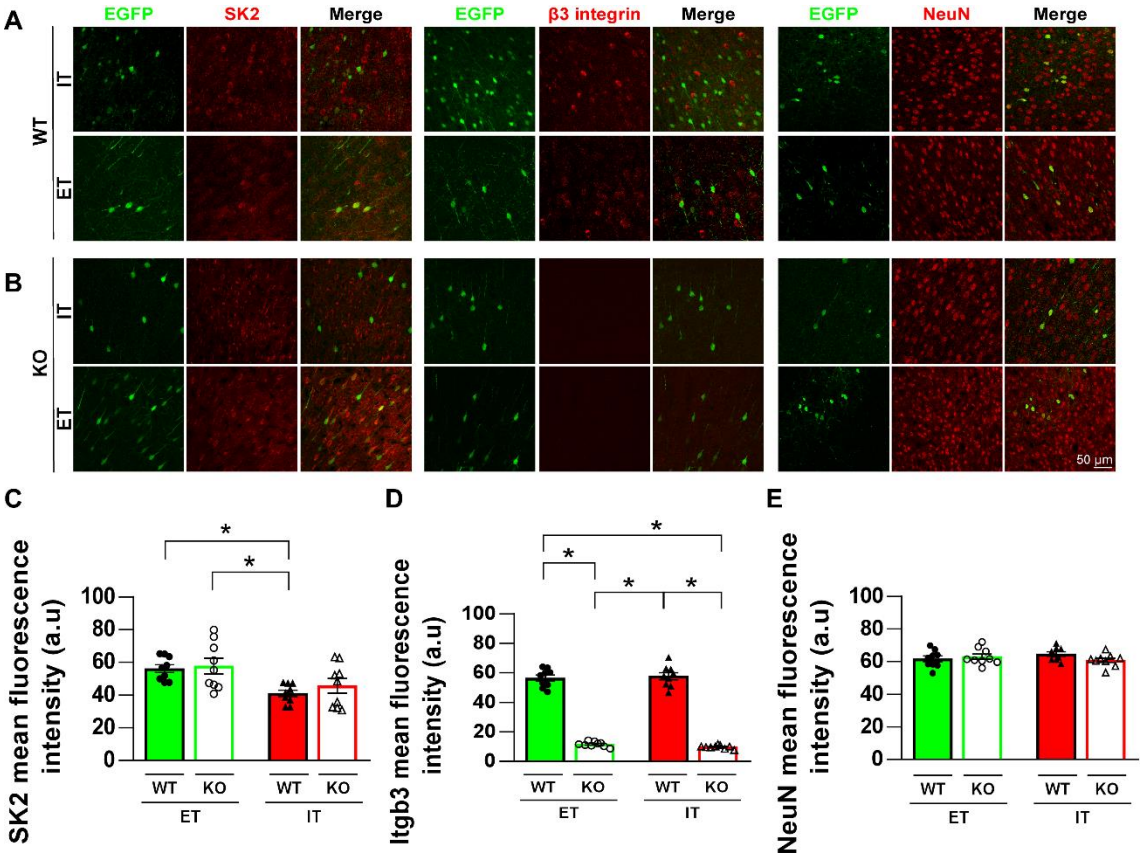

Fig.9 Immunostatining for SK channels, β3 integrin and NeuN of retrogradely labelled WT and KO ET, WT and KO IT neurons (A). Confocal images of SK2 (left), β3 integrin (middle), NeuN (right) in *Itgb3* KO ET and IT neurons of the layer V mPFC **(B)**. Mean fluorescence intensity (a.u.) for SK2 **(C)** β3 integrin **(D)** NeuN **(E)** (for each genotype and each cell type 3 animals were used. Per each animal 3 slices were immunostained for SK2, 3 for β3 integrin and 3 for NeuN. For SK2 WTET-WTIT, p=0.02, KOET-WTIT p=0.01. For all conditions p<0.0001 Ordinary One-way ANOVA Tukey's multiple comparisons test). Data are displayed as mean ± SEM.

5 Discussion

In the central nervous system (CNS), little is known about integrins, heterodimeric transmembrane receptors for extracellular matrix proteins and counter-receptors on adjacent cells. However, the role of integrins in controlling the Ca^{2+} fluxes has been studied in neuron-enriched primary neocortical cultures (Lin et al., 2008). These studies suggest that the interaction of neocortical neurons with the ECM recruits tyrosine kinase pathways and stimulates Ca^{2+} influx possibly through both voltage dependent and independent receptors, such as Cav channels, NMDARs and Ca^{2+} release from intracellular stores. Indeed, integrin ligands containing RGD motifs were able to produce changes in neuronal excitability and Ca^{2+} fluxes within minutes (Lin et al., 2008; Wildering et al., 2002). In particular, glutamate receptors turned out to be a target of integrin dependent regulation (Gall and Lynch, 2004). Many integrin subunits are expressed in the CNS, where some, such as β3, are enriched at synapses (Kerrisk et al., 2014). Previous studies, using RGD peptides and KO models, have shown that the β3 integrin subunit is important for synaptic transmission and plasticity in vitro. This integrin has been recognized as mediator of homeostatic synaptic plasticity for its capability to regulate AMPARs at the PSD (Cingolani et al., 2008; McGeachie et al., 2011), important for the restoring of neuronal excitability upon a deprivation of network activity (Dityatev et al., 2010; Park and Goda, 2016).

SK channels can regulate the intrinsic excitability of a neuron, the firing patterns and spike-frequency adaptation (Adelman et al., 2012; Stocker, 2004). Interestingly, in some neurons there is more than one functional population of SK channels, which can be coupled to different Ca^{2+} sources (Adelman et al., 2012). Despite the variability in the coupling of Cav channels and SK channels, in the same neuron there is distinct and specific coupling of Ca^{2+} channels to different Ca^{2+}-activated K^+ channels. The Ca^{2+}

influx via transmitter-gated ion channels can also activate SK channels, thereby modulating neurotransmission. To notice, the modification of neuronal response to synaptic activity might be influenced not only by alteration in synaptic strength, but also by intrinsic excitability. SK channel activity that contributes to the AHP by shaping intrinsic excitability is also subject to activity-dependent plasticity.

Various aspects of neuronal development are regulated through Ca^{2+} influx, defined by different spatio-temporal patterns depending on the developmental stage, such as the proliferation of neural progenitors, neuronal migration, axon guidance, neurotransmitter and receptor specification, and synapse formation (Dave and Bordey, 2009; Nacher and McEwen, 2006; Rosenberg and Spitzer, 2011; Spitzer, 2006). Dysregulation of these processes can lead to impaired neuronal connectivity and increased risk for several neurodevelopmental pathologies, including ASD (Geschwind and Levitt, 2007; McGlashan and Hoffman, 2000). Several studies in mouse models have found different areas of the brain to be affected by ASD, such as sensory, prefrontal, hippocampal, cerebellar, and striatal regions, as well as the circuits that connect them (Golden et al., 2018). Among all these brain regions, this study was focused on the medial prefrontal cortex, with particular attention on glutamatergic pyramidal neurons ET and IT in LV, also found to be implicated in ASD (Shepherd, 2013). The circuits in which these two neuron types are involved in are different and complex, due to their ubiquitous distribution across the cortex. IT neurons have ipsi- or bilaterally corticocortical (CCor) and corticostriatal (CCstr) projections. ET neurons project to brainstem and in some cases also to spinal cord, with branches to ipsilateral cortex and numerous subregions; however, their intracerebral axons do not cross the corpus callosum or other commissures to the contralateral hemisphere. ET neurons are highly multiprojectional, capable of sending their branches to many subcortical areas. Among all, the striatum is the only subcortical

area that receives both IT (bilaterally) and PT (ipsilaterally) inputs. The neural circuits in which ET and IT neurons are participating can be influenced by neuromodulation, indeed the same circuits could be reconfigured by neuromodulators to perform diverse computation. Four modulatory systems are particularly important in the cortex, noradrenergic inputs from the locus ceruleus, dopaminergic input from the ventral tegmental area, 5-hydroxytryptamine (5-HT) input from the dorsal raphe and cholinergic input from the nucleus basalis. Several studies indicate that noradrenaline might regulate the corticostriatal output selectively via the PT pathway (Dembrow et al., 2010; Shepherd, 2013). On the other end, there are evidences of IT specificity for dopamine due to the expression of D1 and D2 receptors in these neurons, although recent studies have also found the expression of the D2 receptor in ET neurons (Gee et al., 2012). 5-HT might also have a preference for IT over ET neurons, appearing complementary to noradrenaline neuromodulation. The specificity of acetylcholine effects is yet to be understood, although in a recent study it has been observed a specific effect of cholinergic agonist in ET, but not IT neurons (Shepherd, 2013). We are still a long way from comprehending how these neuromodulatory systems operate together in a dynamic and coordinated manner. More studies are needed to address how neuromodulation shapes the function of these circuits also during behaviour. The accessible knowledge suggests that IT and ET neurons have a different roles in cognitive and motor functions, such as action selection, motor control, sequence learning and habit formation. These evidence reveal their involvement in a spectrum of neurological and neuropsychiatric disorders, including ASD (Shepherd, 2013). ASD is a neurodevelopment disorder and different aspects of the neuronal development are regulated by early electrical activity and calcium influx. SK channels regulate action potential firing and shape calcium influx through feedback regulation. For all these reasons and for the discovery in my laboratory of the protein-

protein interaction between β3 integrin and SK channels (unpublished data), I characterized their interplay, analysing the intrinsic excitability and their levels of expression specifically in ET and IT neurons and in their Itgb3 KO counterparts. The hypothesis is that β3 integrin plays an important role during the development interacting with SK channels; therefore, impairments of β3 integrin might lead to a decrease of SK channels functions, which could be linked to development of ASD.

The remarkable variety in genetics, connectivity and functional features of ET and IT LV pyramidal neurons of the mPFC places an organized structure for subtype-specific contributions to nervous system disorder, such as epilepsy, ALS, and ASD. For example, in a study conducted in mouse models of ASD the functional expression of several ion channels was altered in LV ET, but not in IT, neurons (Zhang et al., 2014).

In this study it has been found that the expression of SK channels was higher in LV ET than IT neurons. Both neurons showed a considerable difference in the intrinsic properties, ET neurons resonate at high frequencies (2-6Hz), with approximately low input resistance and need more current to elicit the first APs. IT neurons resonate at low frequencies (0.5-2Hz), with approximately high input resistance and need less current to elicit the first APs (Dembrow and Johnston, 2014; Dembrow et al., 2010) and Table1. Unexpectedly, the Cm was the only passive property that significantly changed between the WT and Itgb3 KO ET neurons. It was higher in Itgb3 KO ET than WT neurons meaning that the absence of β3 integrin might have an effect on their membrane capacitance, which is proportional to the membrane surface area. Moreover, differences of the Cm were also found between ET and IT neurons, the Cm was higher in IT than ET neurons, and it is exciting to speculate that the reduced levels of SK channels expression could lead to an increase of the membrane surface area and of the Cm in IT neurons compared to ET neurons.

The amplitude of the apamin SK-mediated current was bigger in WT ET neurons when compared to both IT and Itgb3 KO ET neurons, while the effect of the SK-activator, NS309, was quite similar in all conditions under analysis. ET neurons have a bigger apamin SK-mediated current due to higher expression levels of SK channels, than IT. On the other hand, Itgb3 KO ET neurons present the same expression levels of SK channels than WT ET; therefore, the reduction of the apamin SK-mediated current might be due to a reduction of SK channels function, through less Ca^{2+} influx caused by the absence of β3 integrin subunit. Among the kinetic properties analysed, also the time of the peak was different between ET and IT neurons, albeit similar to the Itgb3 KO counterparts probably due to a Ca^{2+}-independent mechanisms. ET neurons were faster to reach the maximal activation of SK channels compared to IT neurons. This behaviour could suggest that the SK channels are better activated in ET than IT neurons, most likely because the Ca^{2+} sources are closer to SK channels in ET than IT neurons. This assumption could be proven by analysing the effect of NS309 on SK channels. NS309 is a positive modulator of SK channels and its application increases their sensitivity to intracellular calcium (Strobaek et al., 2004). Therefore, if in ET neurons the Ca^{2+} sources are closer to SK channels, the effect of NS309 should be smaller than the one in IT neurons, where hypothetically the Ca^{2+} sources are far from SK channels. The experiments here performed with NS309 are not yet completely exhaustive to understand the abilities of calcium buffering in ET and IT neurons. Upon apamin application, an increase of the number of action potentials (nAPs) and of the firing frequency would be expected, since SK channels are responsible for the mI_{AHP} (Stocker, 2004). Here, it was observed a significant increase of the nAPs in ET and IT neurons, found to be not significant in Itgb3 KO ET and IT neurons, when apamin was applied. Moreover, in the control the nAPs was significantly reduced in Itgb3 KO ET neurons than the WT ET. These findings indicate that the nAPs are dependent on

the complex β3 integrin-SK channels in ET neurons, but not in IT. The firing frequency was increased for all conditions when apamin was applied, although with no statistical significance, suggesting SK channels are not implicated in the overall regulation of firing frequency in these neurons. Most interesting was the effect on the SFA. With the presence of apamin the SFA should decrease, since SK channels are responsible for generating the phenomenon of SFA (Sah, 1996). Unexpectedly, an increase of the spike-frequency adaptation was observed with apamin, only in ET while no effect was recorded for IT neurons. The effect of apamin on SFA is debated in literature. For example, in basolateral amygdala projection neurons, application of apamin reduced SFA (Power and Sah, 2008). Instead, in spinal motoneurones for steady-state firing frequencies < 30 Hz, adaptation ratios were greater in the presence of apamin compared to control conditions, while for steady-state firing frequencies > 30 Hz, there was no significant difference between adaptation ratios in control and under apamin. These data showed that the AHP actually limits SFA at low steady-state firing frequencies. In comparison, at high steady-state firing frequencies the AHP had no effect on SFA (Miles et al., 2005).

In our study, the singular behavior of ET and IT neurons could be due to the distance between the Ca^{2+} sources and the SK channels. It is possible that in ET neurons, the Ca^{2+} sources are closer to SK channels, therefore the SK channels are rapidly activated by the first APs. This hypothesis could be tested by using the positive modulator NS309 and observing how the firing of ET and IT neurons could be affected by its application. In IT neurons a different behavior is observed, in control conditions these neurons adapt more than ET, as described in the literature (Dembrow et al., 2010), whereas with the presence of apamin there is no effect. It might be possible that the greater SFA observed in IT neurons is due to the slow Ca^{2+}-activated K^+ current (sI_{AHP}). The sI_{AHP} is responsible of the late phase of spike frequency adaptation, reduces the action potential firing and most

of all is apamin-insensitive (Stocker, 2004). This behavior indeed might fit with the higher SFA found in IT than ET neurons in the control, while in the presence of apamin no effect has been reported in IT neurons. In summary, I found that SK channels are responsible for the adaptation in ET neurons, but not in IT neurons. This difference might be due to the higher level of SK channels expression in ET than IT neurons and to the closer proximity of Ca^{2+} sources and SK channels in ET than IT neurons.

Moreover, it has been reported that the spike-time precision of the neuronal firing might depend on SK channels (Stocker, 2004). To test if the spike time precision was different in the IT vs ET neurons or affected by the lack of Itgb3, we calculated the coefficient of variation of the neuronal firing. We observed an increase in the firing variability in LV Itgb3 KO ET neurons, although more experiments are needed for statistical validity. The presence of apamin did not affect wild-type ET or any IT neurons, suggesting that for these neurons the firing precision is not modulated by SK channels.

Previous and unpublished immunohistochemistry data from our lab confirmed the data from in situ hybridizations (Allen Brain atlas) that the β3 integrin subunit is expressed in LV pyramidal neurons of the mPFC, where also SK channels are present (Gymnopoulos et al., 2014; Sailer et al., 2004). Taking the advantage of the different axonal projection targets to label ET and IT neurons, we could analyse the expression of β3 integrin and SK channels separately in two subpopulations of LV pyramidal neurons of mPFC. These experiments were crucial to better understand the differences found of the mI_{AHP} between ET and IT and between WT ET and Itgb3 KO ET neurons. In line with a bigger mI_{AHP} found in WT ET than Itgb3 KO ET and IT neurons, the expression of SK channels was higher in ET than IT neurons, whereas there were no changes for the Itgb3 KO counterparts. In contrast to SK2 levels, the β3 integrin level of expression was the same for ET and IT neurons. These results can explain the differences between ET and IT

neurons, but not between WT ET and Itgb3 KO ET neurons. For the former, it is possible that the bigger SK-mediated current is due to an increased expression of SK channels, for the latter more investigations need to be done, although it might be possible that the absence of β3 integrin is not influencing the expression of SK channels, but their activation or trafficking.

Among all the analysis performed, no differences have been found between Itgb3 KO and WT IT neurons, suggesting that for this neuron subpopulation it is not relevant the interaction between β3 integrin and SK channels, which are also less expressed and have a small current.

It is possible that the differences found between ET and IT neurons are mirroring the highly complex connectivity in which they are involved. They connect different areas of the brain, implicated in different functions, behaviours and regulated by specific neuromodulators. Likely, the β3-SK interplay is more important for the functional activity of ET than IT dependent circuits.

From this study, compelling evidences are provided for the different role that SK channels could play in the two neuron subpopulations from the correlation between the different mI_{AHP} and the level of SK channels expressions found to be unique in ET and IT neurons. Indeed, if we consider that some ASD-mutations were found to converge exactly in these neurons, where the interaction β3 integrin-SK channels has been analysed, it is exciting to speculate that ET neurons are more prone to develop some impairment in their normal activity, partly because of a dysfunction of the interaction β3 integrin-SK channels.

6 Conclusions and future perspectives

In this work, I provide evidence that the interplay between β3 integrin and SK channels plays important roles in ET pyramidal neurons of the layer V mPFC and that ablation of this integrin leads to impairment of their functional activity.

However, I did not find impairment in IT neurons when the β3 integrin was deleted. To notice, ET and IT neurons have different projection targets that allow them to participate in separate neuronal networks controlling different behaviors (Dembrow and Johnston, 2014). As future experiments, it will be interesting to analyze specific ASD-related behaviors, dependent on ET and IT circuits in *Itgb3* KO mice to have a complete overview of the role of β3 integrin-SK channels interaction.

Crucial findings have been the correlations between the mI_{AHP} observed in ET and IT neurons and their expression levels of SK channels. However, no correlations were found in *Itgb3* KO ET neurons between the mI_{AHP} observed and the expression levels of SK channels. In this context, more experiments need to be done to understand this is the case.

Lastly, β3 integrin is implicated in the control of homeostatic synaptic plasticity whereas, SK channels control intrinsic excitability, which is important to homeostatic adaptations. Thus, it would be exciting to investigate how their interaction could shape the homeostatic intrinsic plasticity.

7 Acknowledgements

Spero di aver ringraziato in modo opportuno tutte le persone che mi sono state vicine durante questo intenso percorso.

Vorrei ringraziare il mio supervisore Lorenzo Cingolani, per avermi trasmesso una così grande conoscenza scientifica. Lo ringrazio per la sua pazienza, presenza e supporto. In questi anni il contatto diretto con lui mi ha dato l'opportunità di arricchirmi e di vedere le cose in modo diverso. Farò tesoro dei suoi insegnamenti per la mia futura crescita professionale.

I would like to thank "my postdocs" Agnes Thalhammer and Fanny Jaudon. I would like to thank Agnes for all the suggestions and teachings. I like your passion for science, your being so interactive during lab meetings and your critical thinking. I thank Fanny for your teachings and for having worked side by side. I admire your endless patience, kindness and availability. I thank Lucia Celora for giving me the opportunity to teach electrophysiology for the first time. I thank Eduardo Morais for his support during the first years of my PhD. Thank you for your contribution to my scientific growth.

Vorrei ringraziare il Prof. Fabio Benfenati, per la sua disponibilità e supporto. Lo ringrazio per l'ambiente interdisciplinare presente nel suo dipartimento, per tutti i lab meetings, seminars e retreats. Sono stati degli anni scientificamente stimolanti.

Vorrei ringraziare i miei compagni di dottorato: Assia, Antonio, Matteo e anche Sabi. Durante questi anni abbiamo condiviso molti momenti, siamo cresciuti e abbiamo instaurato una bella amicizia. In particolare ringrazio Assia, con la quale ho condiviso casa per gran parte di questa esperienza, questo ci ha dato l'occasione di instaurare un rapporto più profondo e intenso. Ti ringrazio per le mille chiacchierate, per gli sfoghi, per la comprensione e pazienza.

Vorrei ringraziare tutte le persone dell'NSYN, presenti e passati, dottorandi e postdoc, ricercatori e amministrativi. È stato bello potervi conoscere tutti e condividere tutti i giorni di lavoro di questi ultimi anni. In particolare ringrazio l'amministrazione per l'enorme disponibilità e pazienza che hanno avuto con me. Ringrazio Giorgio per i suoi mille consigli, per il tempo dedicatomi e per avermi ascoltata e supportata nei momenti difficili.

Ringrazio il gruppo della pallavolo, giocare con voi è stato salutare in tutti i sensi e mi ha aiutata ad affrontare questo percorso con più carica e brio.

Vorrei ringraziare Monia ed Ana, per aver instaurato una così bella amicizia con loro. Ringrazio Monia per tutti i film, le cene e i momenti passati insieme, sei stata veramente cruciale per me in questi anni. Il retro di Gelatina è il mio momento felice con te. Ringrazio Ana per tutte le chiacchierate di mattina in cucina, per la nostra passione per il dolce e per essere stata una coinquilina fantastica.

Ringrazio "le storiche", è bello sapere che c'è una sezione per voi fissa e costante. Nonostante la distanza siamo state capaci di affrontare tutte le difficoltà che si sono presentate e di bilanciare il nostro rapporto. Vi ringrazio per esserci, sempre.

Ringrazio tutta la mia famiglia, in particolare i miei genitori per la loro costante presenza, forza e supporto. Siete delle persone fantastiche! Ringrazio mio fratello Raffi, anche lui sempre presente e pronto a consigliarmi il meglio, sono stracontenta e fiera di avere un fratello come te. Ringrazio il mio "Orco" perché nei momenti difficili è sempre stato pronto a ricordarmi di essere forte, di combattere e di tenere gli occhi aperti. Ringrazio anche mia zia, zio e cugini per il supporto continuo, nonostante la distanza.

Durante questi anni una persona per me speciale è venuta a mancare, una donna forte, invincibile, guerriera, gentile e sempre disponibile per gli altri. La sua severità è stato uno

degli ingredienti che mi ha fatta crescere e diventare ciò che sono. Grazie nonna per “o’ piezz e femmn” che sei stato.

Ringrazio il mio Ghirottino per essere stato al mio fianco, per la tua bontà e capacità di essere sempre positivo. Ti ho ammirato tanto per questo, ma soprattutto perché il tuo sorriso mi ha aiutata ad affrontare la vita con occhi diversi. Ti ringrazio perché in questi due anni mi hai dato una mano ogni volta che ne avevo bisogno, sei sempre stato presente, nei momenti belli e brutti e questo ci ha fatti crescere ed arrivare ad instaurare un bellissimo rapporto, del quale ne sono tanto fiera e soddisfatta. Grazie per aver riportato sempre il sole, per le serate passate su MATLAB, per tutte le cene preparate da te e per tutti i disegnini fantabiologici fatti sullo scottex da cucina. Grazie per aver creduto in me quando io stessa avevo dei dubbi, ma più di tutto grazie per avermi aiutato a perseguire i miei sogni. Spero di avere ancora l’opportunità di crescere insieme con te ed intanto porto con me i nostri “100 elefanti, 1000 tartarughe e una foca”. Thanks my love.

8 Bibliography

Adelman, J.P., Maylie, J., and Sah, P. (2012). Small-conductance Ca2+-activated K+ channels: form and function. Annu Rev Physiol *74*, 245-269.

Alcamo, E.A., Chirivella, L., Dautzenberg, M., Dobreva, G., Farinas, I., Grosschedl, R., and McConnell, S.K. (2008). Satb2 regulates callosal projection neuron identity in the developing cerebral cortex. Neuron *57*, 364-377.

Allen, D., Fakler, B., Maylie, J., and Adelman, J.P. (2007). Organization and regulation of small conductance Ca2+-activated K+ channel multiprotein complexes. The Journal of neuroscience : the official journal of the Society for Neuroscience *27*, 2369-2376.

Alvina, K., Ellis-Davies, G., and Khodakhah, K. (2009). T-type calcium channels mediate rebound firing in intact deep cerebellar neurons. Neuroscience *158*, 635-641.

Anastasiades, P.G., Marlin, J.J., and Carter, A.G. (2018). Cell-Type Specificity of Callosally Evoked Excitation and Feedforward Inhibition in the Prefrontal Cortex. Cell reports *22*, 679-692.

Anderson, C.T., Sheets, P.L., Kiritani, T., and Shepherd, G.M.G. (2010). Sublayer-specific microcircuits of corticospinal and corticostriatal neurons in motor cortex. Nature neuroscience *13*, 739-U116.

Arcangeli, A., and Becchetti, A. (2006). Complex functional interaction between integrin receptors and ion channels. Trends in cell biology *16*, 631-639.

Arcangeli, A., and Becchetti, A. (2010). Integrin structure and functional relation with ion channels. Adv Exp Med Biol *674*, 1-7.

Arcangeli, A., Becchetti, A., Mannini, A., Mugnai, G., De Filippi, P., Tarone, G., Del Bene, M.R., Barletta, E., Wanke, E., and Olivotto, M. (1993). Integrin-mediated neurite outgrowth in neuroblastoma cells depends on the activation of potassium channels. J Cell Biol *122*, 1131-1143.

Arima, J., Matsumoto, N., Kishimoto, K., and Akaike, N. (2001). Spontaneous miniature outward currents in mechanically dissociated rat Meynert neurons. The Journal of physiology *534*, 99-107.

Arlotta, P., Molyneaux, B.J., Chen, J., Inoue, J., Kominami, R., and Macklis, J.D. (2005). Neuronal subtype-specific genes that control corticospinal motor neuron development in vivo. Neuron *45*, 207-221.

Arnaout, M.A., Goodman, S.L., and Xiong, J.P. (2007). Structure and mechanics of integrin-based cell adhesion. Current opinion in cell biology *19*, 495-507.

Arnaout, M.A., Mahalingam, B., and Xiong, J.P. (2005). Integrin structure, allostery, and bidirectional signaling. Annual review of cell and developmental biology *21*, 381-410.

Baker, A., Kalmbach, B., Morishima, M., Kim, J., Juavinett, A., Li, N., and Dembrow, N. (2018). Specialized Subpopulations of Deep-Layer Pyramidal Neurons in the Neocortex: Bridging Cellular Properties to Functional Consequences. Journal of Neuroscience *38*, 5441-5455.

Becchetti, A., Pillozzi, S., Morini, R., Nesti, E., and Arcangeli, A. (2010a). New insights into the regulation of ion channels by integrins. International review of cell and molecular biology *279*, 135-190.

Becchetti, A., Pillozzi, S., Morini, R., Nesti, E., and Arcangeli, A. (2010b). New Insights into the Regulation of Ion Channels by Integrins. Int Rev Cel Mol Bio *279*, 135-190.

Bixby, J.L., and Harris, W.A. (1991). Molecular mechanisms of axon growth and guidance. Annual review of cell biology *7*, 117-159.

Blatz, A.L., and Magleby, K.L. (1986). Single apamin-blocked Ca-activated K+ channels of small conductance in cultured rat skeletal muscle. Nature *323*, 718-720.

Blaustein, M.P. (1988). Calcium transport and buffering in neurons. Trends in neurosciences *11*, 438-443.

Bloodgood, B.L., and Sabatini, B.L. (2007). Nonlinear regulation of unitary synaptic signals by CaV(2.3) voltage-sensitive calcium channels located in dendritic spines. Neuron *53*, 249-260.
Bos, J.L. (2005). Linking Rap to cell adhesion. Current opinion in cell biology *17*, 123-128.
Cabodi, S., Di Stefano, P., Leal Mdel, P., Tinnirello, A., Bisaro, B., Morello, V., Damiano, L., Aramu, S., Repetto, D., Tornillo, G.*, et al.* (2010). Integrins and signal transduction. Adv Exp Med Biol *674*, 43-54.
Campbell, I.D., and Humphries, M.J. (2011). Integrin structure, activation, and interactions. Cold Spring Harbor perspectives in biology *3*.
Cao, Y., Dreixler, J.C., Roizen, J.D., Roberts, M.T., and Houamed, K.M. (2001). Modulation of recombinant small-conductance Ca(2+)-activated K(+) channels by the muscle relaxant chlorzoxazone and structurally related compounds. The Journal of pharmacology and experimental therapeutics *296*, 683-689.
Carter, M.D., Shah, C.R., Muller, C.L., Crawley, J.N., Carneiro, A.M., and Veenstra-Vanderweele, J. (2011). Absence of preference for social novelty and increased grooming in integrin beta3 knockout mice: Initial studies and future directions. Autism Res *4*, 57-67.
Catterall, W.A. (2010). Ion channel voltage sensors: structure, function, and pathophysiology. Neuron *67*, 915-928.
Chan, C.S., Weeber, E.J., Kurup, S., Sweatt, J.D., and Davis, R.L. (2003). Integrin requirement for hippocampal synaptic plasticity and spatial memory. The Journal of neuroscience : the official journal of the Society for Neuroscience *23*, 7107-7116.
Chan, C.S., Weeber, E.J., Zong, L., Fuchs, E., Sweatt, J.D., and Davis, R.L. (2006). Beta 1-integrins are required for hippocampal AMPA receptor-dependent synaptic transmission, synaptic plasticity, and working memory. The Journal of neuroscience : the official journal of the Society for Neuroscience *26*, 223-232.
Chavis, P., and Westbrook, G. (2001). Integrins mediate functional pre- and postsynaptic maturation at a hippocampal synapse. Nature *411*, 317-321.
Cherubini, A., Hofmann, G., Pillozzi, S., Guasti, L., Crociani, O., Cilia, E., Di Stefano, P., Degani, S., Balzi, M., Olivotto, M.*, et al.* (2005). Human ether-a-go-go-related gene 1 channels are physically linked to beta1 integrins and modulate adhesion-dependent signaling. Molecular biology of the cell *16*, 2972-2983.
Christophe, E., Doerflinger, N., Lavery, D.J., Molnar, Z., Charpak, S., and Audinat, E. (2005). Two populations of layer v pyramidal cells of the mouse neocortex: development and sensitivity to anesthetics. Journal of neurophysiology *94*, 3357-3367.
Cingolani, L.A., and Goda, Y. (2008). Differential involvement of beta3 integrin in pre- and postsynaptic forms of adaptation to chronic activity deprivation. Neuron glia biology *4*, 179-187.
Cingolani, L.A., Gymnopoulos, M., Boccaccio, A., Stocker, M., and Pedarzani, P. (2002). Developmental regulation of small-conductance Ca2+-activated K+ channel expression and function in rat Purkinje neurons. The Journal of neuroscience : the official journal of the Society for Neuroscience *22*, 4456-4467.
Cingolani, L.A., Thalhammer, A., Yu, L.M., Catalano, M., Ramos, T., Colicos, M.A., and Goda, Y. (2008). Activity-dependent regulation of synaptic AMPA receptor composition and abundance by beta3 integrins. Neuron *58*, 749-762.
Cingolani, L.A., Vitale, C., and Dityatev, A. (2019). Intra- and Extracellular Pillars of a Unifying Framework for Homeostatic Plasticity: A Crosstalk Between Metabotropic Receptors and Extracellular Matrix. Front Cell Neurosci *13*.
Coetzee, W.A., Amarillo, Y., Chiu, J., Chow, A., Lau, D., McCormack, T., Moreno, H., Nadal, M.S., Ozaita, A., Pountney, D.*, et al.* (1999). Molecular diversity of K+ channels. Annals of the New York Academy of Sciences *868*, 233-285.
Crandall, S.R., Patrick, S.L., Cruikshank, S.J., and Connors, B.W. (2017). Infrabarrels Are Layer 6 Circuit Modules in the Barrel Cortex that Link Long-Range Inputs and Outputs. Cell reports *21*, 3065-3078.

Critchley, D.R. (2000). Focal adhesions - the cytoskeletal connection. Current opinion in cell biology *12*, 133-139.
Critchley, D.R., and Gingras, A.R. (2008). Talin at a glance. Journal of cell science *121*, 1345-1347.
Cull-Candy, S., Brickley, S., and Farrant, M. (2001). NMDA receptor subunits: diversity, development and disease. Current opinion in neurobiology *11*, 327-335.
Dembrow, N., and Johnston, D. (2014). Subcircuit-specific neuromodulation in the prefrontal cortex. Frontiers in neural circuits *8*.
Dembrow, N.C., Chitwood, R.A., and Johnston, D. (2010). Projection-specific neuromodulation of medial prefrontal cortex neurons. The Journal of neuroscience : the official journal of the Society for Neuroscience *30*, 16922-16937.
Dembrow, N.C., Zemelman, B.V., and Johnston, D. (2015). Temporal dynamics of L5 dendrites in medial prefrontal cortex regulate integration versus coincidence detection of afferent inputs. The Journal of neuroscience : the official journal of the Society for Neuroscience *35*, 4501-4514.
Doherty, P., Ashton, S.V., Moore, S.E., and Walsh, F.S. (1991). Morphoregulatory activities of NCAM and N-cadherin can be accounted for by G protein-dependent activation of L- and N-type neuronal Ca2+ channels. Cell *67*, 21-33.
Dohn, M.R., Kooker, C.G., Bastarache, L., Jessen, T., Rinaldi, C., Varney, S., Mazalouskas, M.D., Pan, H., Oliver, K.H., Velez Edwards, D.R.*, et al.* (2017). The Gain-of-Function Integrin beta3 Pro33 Variant Alters the Serotonin System in the Mouse Brain. The Journal of neuroscience : the official journal of the Society for Neuroscience *37*, 11271-11284.
Faber, E.S., Delaney, A.J., Power, J.M., Sedlak, P.L., Crane, J.W., and Sah, P. (2008). Modulation of SK channel trafficking by beta adrenoceptors enhances excitatory synaptic transmission and plasticity in the amygdala. The Journal of neuroscience : the official journal of the Society for Neuroscience *28*, 10803-10813.
Faber, E.S., Delaney, A.J., and Sah, P. (2005). SK channels regulate excitatory synaptic transmission and plasticity in the lateral amygdala. Nature neuroscience *8*, 635-641.
Faber, E.S., and Sah, P. (2003). Ca2+-activated K+ (BK) channel inactivation contributes to spike broadening during repetitive firing in the rat lateral amygdala. The Journal of physiology *552*, 483-497.
Fakler, B., and Adelman, J.P. (2008). Control of K(Ca) channels by calcium nano/microdomains. Neuron *59*, 873-881.
Ferreira, A.N., Yousuf, H., Dalton, S., and Sheets, P.L. (2015). Highly differentiated cellular and circuit properties of infralimbic pyramidal neurons projecting to the periaqueductal gray and amygdala. Front Cell Neurosci *9*.
Fiorillo, C.D., and Williams, J.T. (1998). Glutamate mediates an inhibitory postsynaptic potential in dopamine neurons. Nature *394*, 78-82.
Gall, C.M., and Lynch, G. (2004). Integrins, synaptic plasticity and epileptogenesis. Adv Exp Med Biol *548*, 12-33.
Geschwind, D.H., and Levitt, P. (2007). Autism spectrum disorders: developmental disconnection syndromes. Current opinion in neurobiology *17*, 103-111.
Guan, D., Armstrong, W.E., and Foehring, R.C. (2015). Electrophysiological properties of genetically identified subtypes of layer 5 neocortical pyramidal neurons: Ca(2)(+) dependence and differential modulation by norepinephrine. Journal of neurophysiology *113*, 2014-2032.
Gulledge, A.T., and Stuart, G.J. (2005). Cholinergic inhibition of neocortical pyramidal neurons. The Journal of neuroscience : the official journal of the Society for Neuroscience *25*, 10308-10320.
Gymnopoulos, M., Cingolani, L.A., Pedarzani, P., and Stocker, M. (2014). Developmental mapping of small-conductance calcium-activated potassium channel expression in the rat nervous system. J Comp Neurol *522*, 1072-1101.
Harburger, D.S., and Calderwood, D.A. (2009). Integrin signalling at a glance. Journal of cell science *122*, 159-163.

Hattox, A.M., and Nelson, S.B. (2007). Layer V neurons in mouse cortex projecting to different targets have distinct physiological properties. Journal of neurophysiology *98*, 3330-3340.
Hille, B. (1986). Ionic channels: molecular pores of excitable membranes. Harvey lectures *82*, 47-69.
Hirai, Y., Morishima, M., Karube, F., and Kawaguchi, Y. (2012). Specialized Cortical Subnetworks Differentially Connect Frontal Cortex to Parahippocampal Areas. Journal of Neuroscience *32*, 1898-1913.
Hirschberg, B., Maylie, J., Adelman, J.P., and Marrion, N.V. (1998). Gating of recombinant small-conductance Ca-activated K+ channels by calcium. The Journal of general physiology *111*, 565-581.
Huang, Z., Shimazu, K., Woo, N.H., Zang, K., Muller, U., Lu, B., and Reichardt, L.F. (2006). Distinct roles of the beta 1-class integrins at the developing and the mature hippocampal excitatory synapse. J Neurosci *26*, 11208-11219.
Hutcheon, B., and Yarom, Y. (2000). Resonance, oscillation and the intrinsic frequency preferences of neurons. Trends in neurosciences *23*, 216-222.
Hutsler, J.J., and Zhang, H. (2010). Increased dendritic spine densities on cortical projection neurons in autism spectrum disorders. Brain research *1309*, 83-94.
Hynes, R.O. (2002). Integrins: bidirectional, allosteric signaling machines. Cell *110*, 673-687.
Ingber, D.E., Prusty, D., Frangioni, J.V., Cragoe, E.J., Jr., Lechene, C., and Schwartz, M.A. (1990). Control of intracellular pH and growth by fibronectin in capillary endothelial cells. The Journal of cell biology *110*, 1803-1811.
Ishii, T.M., Silvia, C., Hirschberg, B., Bond, C.T., Adelman, J.P., and Maylie, J. (1997). A human intermediate conductance calcium-activated potassium channel. Proceedings of the National Academy of Sciences of the United States of America *94*, 11651-11656.
Joshi, A., Middleton, J.W., Anderson, C.T., Borges, K., Suter, B.A., Shepherd, G.M.G., and Tzounopoulos, T. (2015). Cell-Specific Activity-Dependent Fractionation of Layer 2/3 -> 5B Excitatory Signaling in Mouse Auditory Cortex. Journal of Neuroscience *35*, 3112-3123.
Kalmbach, B.E., Johnston, D., and Brager, D.H. (2015). Cell-Type Specific Channelopathies in the Prefrontal Cortex of the fmr1-/y Mouse Model of Fragile X Syndrome(1,2,3). Eneuro *2*.
Kerrisk, M.E., Cingolani, L.A., and Koleske, A.J. (2014). ECM receptors in neuronal structure, synaptic plasticity, and behavior. Progress in brain research *214*, 101-131.
Kinnischtzke, A.K., Fanselow, E.E., and Simons, D.J. (2016). Target-specific M1 inputs to infragranular S1 pyramidal neurons. Journal of neurophysiology *116*, 1261-1274.
Kohler, M., Hirschberg, B., Bond, C.T., Kinzie, J.M., Marrion, N.V., Maylie, J., and Adelman, J.P. (1996). Small-conductance, calcium-activated potassium channels from mammalian brain. Science *273*, 1709-1714.
Kramar, E.A., Lin, B., Lin, C.Y., Arai, A.C., Gall, C.M., and Lynch, G. (2004). A novel mechanism for the facilitation of theta-induced long-term potentiation by brain-derived neurotrophic factor. The Journal of neuroscience : the official journal of the Society for Neuroscience *24*, 5151-5161.
Lamy, C., Goodchild, S.J., Weatherall, K.L., Jane, D.E., Liegeois, J.F., Seutin, V., and Marrion, N.V. (2010). Allosteric block of KCa2 channels by apamin. The Journal of biological chemistry *285*, 27067-27077.
Lilja, J., and Ivaska, J. (2018). Integrin activity in neuronal connectivity. Journal of cell science *131*.
Lin, B., Arai, A.C., Lynch, G., and Gall, C.M. (2003). Integrins regulate NMDA receptor-mediated synaptic currents. Journal of neurophysiology *89*, 2874-2878.
Lin, C.Y., Hilgenberg, L.G., Smith, M.A., Lynch, G., and Gall, C.M. (2008a). Integrin regulation of cytoplasmic calcium in excitatory neurons depends upon glutamate receptors and release from intracellular stores. Molecular and cellular neurosciences *37*, 770-780.
Lin, M.T., Lujan, R., Watanabe, M., Adelman, J.P., and Maylie, J. (2008b). SK2 channel plasticity contributes to LTP at Schaffer collateral-CA1 synapses. Nature neuroscience *11*, 170-177.

Lodato, S., Shetty, A.S., and Arlotta, P. (2015). Cerebral cortex assembly: generating and reprogramming projection neuron diversity. Trends in neurosciences *38*, 117-125.
Madison, D.V., and Nicoll, R.A. (1982). Noradrenaline blocks accommodation of pyramidal cell discharge in the hippocampus. Nature *299*, 636-638.
Maingret, F., Coste, B., Hao, J., Giamarchi, A., Allen, D., Crest, M., Litchfield, D.W., Adelman, J.P., and Delmas, P. (2008). Neurotransmitter modulation of small-conductance Ca2+-activated K+ channels by regulation of Ca2+ gating. Neuron *59*, 439-449.
Marrion, N.V., and Tavalin, S.J. (1998). Selective activation of Ca2+-activated K+ channels by co-localized Ca2+ channels in hippocampal neurons. Nature *395*, 900-905.
McGeachie, A.B., Cingolani, L.A., and Goda, Y. (2011). Stabilising influence: integrins in regulation of synaptic plasticity. Neuroscience research *70*, 24-29.
McGlashan, T.H., and Hoffman, R.E. (2000). Schizophrenia as a disorder of developmentally reduced synaptic connectivity. Archives of general psychiatry *57*, 637-648.
Milner, R., and Campbell, I.L. (2002). The integrin family of cell adhesion molecules has multiple functions within the CNS. Journal of neuroscience research *69*, 286-291.
Molyneaux, B.J., Arlotta, P., Menezes, J.R.L., and Macklis, J.D. (2007). Neuronal subtype specification in the cerebral cortex. Nature Reviews Neuroscience *8*, 427-437.
Monaghan, A.S., Benton, D.C., Bahia, P.K., Hosseini, R., Shah, Y.A., Haylett, D.G., and Moss, G.W. (2004). The SK3 subunit of small conductance Ca2+-activated K+ channels interacts with both SK1 and SK2 subunits in a heterologous expression system. The Journal of biological chemistry *279*, 1003-1009.
Morikawa, H., Imani, F., Khodakhah, K., and Williams, J.T. (2000). Inositol 1,4,5-triphosphate-evoked responses in midbrain dopamine neurons. The Journal of neuroscience : the official journal of the Society for Neuroscience *20*, RC103.
Morini, R., and Becchetti, A. (2010). Integrin Receptors and Ligand-Gated Channels. Adv Exp Med Biol *674*, 95-105.
Morishima, M., and Kawaguchi, Y. (2006). Recurrent connection patterns of corticostriatal pyramidal cells in frontal cortex. Journal of Neuroscience *26*, 4394-4405.
Moyer, C.E., Shelton, M.A., and Sweet, R.A. (2015). Dendritic spine alterations in schizophrenia. Neuroscience letters *601*, 46-53.
Muralidharan, B., Khatri, Z., Maheshwari, U., Gupta, R., Roy, B., Pradhan, S.J., Karmodiya, K., Padmanabhan, H., Shetty, A.S., Balaji, C*., et al.* (2017). LHX2 Interacts with the NuRD Complex and Regulates Cortical Neuron Subtype Determinants Fezf2 and Sox11. Journal of Neuroscience *37*, 194-203.
Norris, C.M., Halpain, S., and Foster, T.C. (1998). Reversal of age-related alterations in synaptic plasticity by blockade of L-type Ca2+ channels. The Journal of neuroscience : the official journal of the Society for Neuroscience *18*, 3171-3179.
O'Roak, B.J., Vives, L., Girirajan, S., Karakoc, E., Krumm, N., Coe, B.P., Levy, R., Ko, A., Lee, C., Smith, J.D*., et al.* (2012). Sporadic autism exomes reveal a highly interconnected protein network of de novo mutations. Nature *485*, 246-250.
Oliver, D., Klocker, N., Schuck, J., Baukrowitz, T., Ruppersberg, J.P., and Fakler, B. (2000). Gating of Ca2+-activated K+ channels controls fast inhibitory synaptic transmission at auditory outer hair cells. Neuron *26*, 595-601.
Oswald, M.J., Tantirigama, M.L.S., Sonntag, I., Hughes, S.M., and Empson, R.M. (2013). Diversity of layer 5 projection neurons in the mouse motor cortex. Front Cell Neurosci *7*.
Otsuka, T., and Kawaguchi, Y. (2008). Firing-Pattern-Dependent Specificity of Cortical Excitatory Feed-Forward Subnetworks. Journal of Neuroscience *28*, 11186-11195.
Otsuka, T., and Kawaguchi, Y. (2011). Cell Diversity and Connection Specificity between Callosal Projection Neurons in the Frontal Cortex. Journal of Neuroscience *31*, 3862-3870.
Park, Y.K., and Goda, Y. (2016). Integrins in synapse regulation. Nature reviews Neuroscience *17*, 745-756.

Pasquereau, B., DeLong, M.R., and Turner, R.S. (2016). Primary motor cortex of the parkinsonian monkey: altered encoding of active movement. Brain *139*, 127-143.
Pasquereau, B., and Turner, R.S. (2011). Primary Motor Cortex of the Parkinsonian Monkey: Differential Effects on the Spontaneous Activity of Pyramidal Tract-Type Neurons. Cerebral cortex *21*, 1362-1378.
Pedarzani, P., McCutcheon, J.E., Rogge, G., Jensen, B.S., Christophersen, P., Hougaard, C., Strobaek, D., and Stocker, M. (2005). Specific enhancement of SK channel activity selectively potentiates the afterhyperpolarizing current I(AHP) and modulates the firing properties of hippocampal pyramidal neurons. The Journal of biological chemistry *280*, 41404-41411.
Pinto, D., Pagnamenta, A.T., Klei, L., Anney, R., Merico, D., Regan, R., Conroy, J., Magalhaes, T.R., Correia, C., Abrahams, B.S.*, et al.* (2010). Functional impact of global rare copy number variation in autism spectrum disorders. Nature *466*, 368-372.
Pozo, K., Cingolani, L.A., Bassani, S., Laurent, F., Passafaro, M., and Goda, Y. (2012). beta3 integrin interacts directly with GluA2 AMPA receptor subunit and regulates AMPA receptor expression in hippocampal neurons. Proceedings of the National Academy of Sciences of the United States of America *109*, 1323-1328.
Ramaswamy, S., and Markram, H. (2015). Anatomy and physiology of the thick-tufted layer 5 pyramidal neuron. Front Cell Neurosci *9*.
Ren, Y., Barnwell, L.F., Alexander, J.C., Lubin, F.D., Adelman, J.P., Pfaffinger, P.J., Schrader, L.A., and Anderson, A.E. (2006). Regulation of surface localization of the small conductance Ca2+-activated potassium channel, Sk2, through direct phosphorylation by cAMP-dependent protein kinase. The Journal of biological chemistry *281*, 11769-11779.
Rock, C., and Apicella, A.J. (2015). Callosal Projections Drive Neuronal-Specific Responses in the Mouse Auditory Cortex. Journal of Neuroscience *35*, 6703-6713.
Rojas-Piloni, G., Guest, J.M., Egger, R., Johnson, A.S., Sakmann, B., and Oberlaender, M. (2017). Relationships between structure, in vivo function and long-range axonal target of cortical pyramidal tract neurons. Nature communications *8*.
Sabatini, B.L., Oertner, T.G., and Svoboda, K. (2002). The life cycle of Ca(2+) ions in dendritic spines. Neuron *33*, 439-452.
Sah, P. (1992). Role of calcium influx and buffering in the kinetics of Ca(2+)-activated K+ current in rat vagal motoneurons. Journal of neurophysiology *68*, 2237-2247.
Sah, P. (1996). Ca(2+)-activated K+ currents in neurones: types, physiological roles and modulation. Trends in neurosciences *19*, 150-154.
Sailer, C.A., Kaufmann, W.A., Marksteiner, J., and Knaus, H.G. (2004). Comparative immunohistochemical distribution of three small-conductance Ca2+-activated potassium channel subunits, SK1, SK2, and SK3 in mouse brain. Molecular and cellular neurosciences *26*, 458-469.
Schumacher, M.A., Crum, M., and Miller, M.C. (2004). Crystal structures of apocalmodulin and an apocalmodulin/SK potassium channel gating domain complex. Structure *12*, 849-860.
Schumacher, M.A., Rivard, A.F., Bachinger, H.P., and Adelman, J.P. (2001). Structure of the gating domain of a Ca2+-activated K+ channel complexed with Ca2+/calmodulin. Nature *410*, 1120-1124.
Seutin, V., Mkahli, F., Massotte, L., and Dresse, A. (2000). Calcium release from internal stores is required for the generation of spontaneous hyperpolarizations in dopaminergic neurons of neonatal rats. Journal of neurophysiology *83*, 192-197.
Sheets, P.L., Suter, B.A., Kiritani, T., Chan, C.S., Surmeier, J., and Shepherd, G.M.G. (2011). Corticospinal-specific HCN expression in mouse motor cortex: I-h-dependent synaptic integration as a candidate microcircuit mechanism involved in motor control. Journal of neurophysiology *106*, 2216-2231.
Shepherd, G.M. (2013). Corticostriatal connectivity and its role in disease. Nat Rev Neurosci *14*, 278-291.

Sourdet, V., Russier, M., Daoudal, G., Ankri, N., and Debanne, D. (2003). Long-term enhancement of neuronal excitability and temporal fidelity mediated by metabotropic glutamate receptor subtype 5. The Journal of neuroscience : the official journal of the Society for Neuroscience *23*, 10238-10248.
Spitzer, N.C. (2006). Electrical activity in early neuronal development. Nature *444*, 707-712.
Staubli, U., Chun, D., and Lynch, G. (1998). Time-dependent reversal of long-term potentiation by an integrin antagonist. The Journal of neuroscience : the official journal of the Society for Neuroscience *18*, 3460-3469.
Staubli, U., Vanderklish, P., and Lynch, G. (1990). An inhibitor of integrin receptors blocks long-term potentiation. Behavioral and neural biology *53*, 1-5.
Stocker, M. (2004). Ca2+-activated K+ channels: molecular determinants and function of the SK family. Nature Reviews Neuroscience *5*, 758-770.
Stocker, M., and Pedarzani, P. (2000). Differential distribution of three Ca(2+)-activated K(+) channel subunits, SK1, SK2, and SK3, in the adult rat central nervous system. Mol Cell Neurosci *15*, 476-493.
Storm, J.F. (1987). Action potential repolarization and a fast after-hyperpolarization in rat hippocampal pyramidal cells. The Journal of physiology *385*, 733-759.
Strassmaier, T., Bond, C.T., Sailer, C.A., Knaus, H.G., Maylie, J., and Adelman, J.P. (2005). A novel isoform of SK2 assembles with other SK subunits in mouse brain. The Journal of biological chemistry *280*, 21231-21236.
Suter, B.A., and Shepherd, G.M.G. (2015). Reciprocal Interareal Connections to Corticospinal Neurons in Mouse M1 and S2. Journal of Neuroscience *35*, 2959-2974.
Thalhammer, A., and Cingolani, L.A. (2014). Cell adhesion and homeostatic synaptic plasticity. Neuropharmacology *78*, 23-30.
Wang, K., Kelley, M.H., Wu, W.W., Adelman, J.P., and Maylie, J. (2015). Apamin Boosting of Synaptic Potentials in CaV2.3 R-Type Ca2+ Channel Null Mice. PloS one *10*, e0139332.
Wegener, K.L., and Campbell, I.D. (2008). Transmembrane and cytoplasmic domains in integrin activation and protein-protein interactions (review). Molecular membrane biology *25*, 376-387.
Wei, A.D., Gutman, G.A., Aldrich, R., Chandy, K.G., Grissmer, S., and Wulff, H. (2005). International Union of Pharmacology. LII. Nomenclature and molecular relationships of calcium-activated potassium channels. Pharmacological reviews *57*, 463-472.
Wildering, W.C., Hermann, P.M., and Bulloch, A.G. (2002). Rapid neuromodulatory actions of integrin ligands. The Journal of neuroscience : the official journal of the Society for Neuroscience *22*, 2419-2426.
Willsey, A.J., Sanders, S.J., Li, M., Dong, S., Tebbenkamp, A.T., Muhle, R.A., Reilly, S.K., Lin, L., Fertuzinhos, S., Miller, J.A*., et al.* (2013). Coexpression networks implicate human midfetal deep cortical projection neurons in the pathogenesis of autism. Cell *155*, 997-1007.
Wilson, C.J. (1987). Morphology and Synaptic Connections of Crossed Corticostriatal Neurons in the Rat. Journal of Comparative Neurology *263*, 567-580.
Xia, X.M., Fakler, B., Rivard, A., Wayman, G., Johnson-Pais, T., Keen, J.E., Ishii, T., Hirschberg, B., Bond, C.T., Lutsenko, S*., et al.* (1998). Mechanism of calcium gating in small-conductance calcium-activated potassium channels. Nature *395*, 503-507.
Xiao, P., Bahr, B.A., Staubli, U., Vanderklish, P.W., and Lynch, G. (1991). Evidence that matrix recognition contributes to stabilization but not induction of LTP. Neuroreport *2*, 461-464.
Xiong, J.P., Stehle, T., Diefenbach, B., Zhang, R., Dunker, R., Scott, D.L., Joachimiak, A., Goodman, S.L., and Arnaout, M.A. (2001). Crystal structure of the extracellular segment of integrin alpha Vbeta3. Science *294*, 339-345.
Xiong, J.P., Stehle, T., Zhang, R., Joachimiak, A., Frech, M., Goodman, S.L., and Arnaout, M.A. (2002). Crystal structure of the extracellular segment of integrin alpha Vbeta3 in complex with an Arg-Gly-Asp ligand. Science *296*, 151-155.

Zhang, Y., Bonnan, A., Bony, G., Ferezou, I., Pietropaolo, S., Ginger, M., Sans, N., Rossier, J., Oostra, B., Le Masson, G.*, et al.* (2014). Dendritic channelopathies contribute to neocortical and sensory hyperexcitability in Fmr1-(/y) mice. Nature neuroscience *17*, 1701-1709.
Zheng, J.Q., and Poo, M.M. (2007). Calcium signaling in neuronal motility. Annual review of cell and developmental biology *23*, 375-404.